Coma Morphology of Jupiter Family Comets

Tony L. Farnham *

Department of Astronomy, University of Maryland, College Park, MD 20742

Abstract

We present a general review of cometary coma morphology, with specific reference to how it used in studies of Jupiter family comets. We introduce the most common features that are seen in gas and dust observations, and summarize of how they are used to infer the properties of the nucleus and coma. We also expand the discussion to cover other topics relating to morphology, including the general shape of the coma (characterized by radial gradient profiles) and spatial maps of the color, albedo and polarization of the dust. We address the pros and cons of the different approaches used in the interpretation and analysis of the features. Finally, we review the results obtained for specific comets and compare the Jupiter family comets to those from other classes.

1 Introduction

Comets are unique among the small bodies of the solar system. Consider that before the first telescopic observations of the heavens in the early 1600s, observations of solar system bodies consisted of the Sun, Moon, five planets—and hundreds of comets. The reason they are so widely represented is their dynamic and active nature. They generate copious amounts of gas and dust, producing the highly visible comae and tails that instilled fear and awe into observers and on occasion even influenced history. However, the sudden appearance of a bright comet was not the only fact that observers found noteworthy. Numerous historical reports of transient "broom stars" or "hairy stars" also go on to describe features, including rays, spikes, needles, beams, smoke and vapor. Reliable records also note variations and changes in the features from night to night and even occasionally within a single night. This transience added to the mystique of comets.

Given the limited resolution of naked eye observations, it is logical to presume that the features described in early observations of comets are the large scale rays and streamers that are

* Corresponding author.
Email address: farnham@astro.umd.edu (Tony L. Farnham).

commonly associated with dust and plasma tails. After the introduction of telescopic observations, reports of elongated and/or asymmetric comae (usually brighter on the sunward side) and different degrees of central condensation became common, suggesting that resolution limits were improving to the point where features such as broad fans could be distinguished from the more extensive tail structures. Robert Hooke, observing comet C/1680 V_1, provides the first description of well-defined features (a fountain of material pointing toward the Sun and then curving away) that can reasonably be attributed to inner coma structures (Kronk, 1999, and references therein). Two years later, Hevelius noted a crooked ray, and Hooke reported seeing a pair of jets, 90° apart and centered on the comet-Sun line, in the first identified periodic comet 1P/Halley.

Historically, Jupiter-family comet (JFC) sightings tend to be unremarkable, because the comets are usually faint, and naked-eye observations only reveal simple, circular comae and short, featureless tails. The first JFC identified with coma structures was probably 2P/Encke, where, on several apparitions between its 1786 discovery and 1838, it is described as having an oval or elongated coma. The 1838 apparition is specifically being identified as having a coma that was elongated in the sunward direction, which is undoubtedly the sunward fan that is commonly associated with this comet (discussed in detail later).

At its most fundamental level, a feature simply represents a spatial variation in the coma, where the environment differs from its surroundings in some manner. In general, these variations are the result of processes relating to the nucleus, or to the interaction of the comet and the solar environment. This intimate relationship links the coma and the nucleus in such a way that features, which are detectable at large distances, can be used to infer properties of the unresolved nucleus. Furthermore, the morphology contains a record of temporal changes that have taken place during the formation of the features. Early on it was discovered that periodic variations and features in the coma could be used to derive rotation periods. Since then, new and exciting techniques have been developed to measure the rotation state, activity of the nucleus, dust and gas properties, and other fundamental properties about the comet.

The intent of this manuscript is to review the different types of coma morphology and to discuss how particular features are observed, interpreted, analyzed and used to derive properties relating to the comet. The common concept of coma morphology tends to focus on the bright jets, fans and arc structures that are typically observed in comet images. We will, of course, address these features, but we will also extend the discussion to include a number of other data types and techniques that are being developed to utilize the coma morphology in different ways. These topics include radial gradient profiles, spatial maps of the color, albedo and polarization of the coma, and comparisons of features seen at different wavelengths. Because the focus is on learning about the nucleus and the coma properties, structures created primarily by interaction with the solar environment will not be addressed in any detail.

We first describe the most common types of coma morphology and address image processing techniques in Section 2. In Section 3 we summarize the two basic schools of thought that

have arisen in studies of coma features, and in Section 4, we describe how coma morphology can be used as a tool to infer the properties of the nucleus and dust. In Section 5 we discuss the morphology observed in Jupiter family comets, and how it compares to that seen in other comets. Finally, we individually discuss some of the more high-profile JFCs in Section 6, with special emphasis on what was learned in the three JFC spacecraft encounters and how those cases can be used to evaluate the capabilities of techniques used in ground-based studies.

2 General Coma Morphology

The importance of morphology in cometary studies is reflected in the fact that feature detections have become increasingly more common over the last 10-20 years, and spatial structures are seen over almost the entire spectrum of wavelengths and with almost every observational technique available. This wealth of data, in both volume and type, has been a valuable tool in studies of morphology, allowing different observations and techniques to help resolve ambiguities in the interpretation.

Many different types of features are seen in comet comae (e.g., Rahe et al., 1969). They can be produced by dust, neutral gas, and ions, all potentially visible in a single image. Structures are seen on spatial scales larger than 10^5 km and as small as a few meters. They can appear as long-term, steady-state formations that persist for months or they can vary on timescales as short as minutes. Singular events that are spontaneous and unpredictable are as common as those that repeat with amazing regularity. They can appear chaotic and disorganized or have symmetric, well-defined shapes. The concept of morphology encompasses simple elongations of the coma as well as the most intricate features seen in high-resolution spacecraft images. It covers brightness variations, color differences, degrees of polarization and temporal changes. Regardless of the specific details, however, each of these characteristics contains information regarding the nucleus and its activity, and studies of coma morphology are geared toward using this information to infer the nucleus properties.

2.1 Classes of Observed Features

Most coma features can be organized into a small number of morphological categories, which are identified here. In the following, we adopt terminology commonly used in the literature, but the use of these terms is intended for descriptive purposes, and does not necessarily imply any particular physical interpretation or formation mechanism.

Coma Shape. The most fundamental type of morphology is the overall shape of the ambient coma. Most comets, when active, tend to exhibit a coma dominated by a diffuse nebulosity surrounding the nucleus. In a large fraction of comets, this diffuse component is all that is ever detected, either because there are no features present, or because they remain unresolved for various reasons. Even in the absence of other features, however, the shape and structure

of the diffuse ambient material can, in itself, be informative. The coma may be elongated and/or asymmetric, with the nucleus offset from the center in any direction. The level of condensation is also variable, with some comets highly condensed and others more diffuse. Variations in brightness (e.g., outbursts), color, or polarization may be seen, and each of these variations provides information about the comet's behavior.

Fans and Jets. The most common type of reported features are fans and jets, which project radially outward from the nucleus. Fans are broad extensions of the coma, frequently exhibiting a wedge or triangular shape (Fig. 1), though in a more general definition, they can range from a narrow triangle to a full hemispheric form. There is no preferred orientation, as they have been observed in the sunward direction, perpendicular to the sun-comet line, and in the tailward direction. Fans also tend to appear long-lived and stable, showing gradual changes over long time scales. Jets—also called spikes, rays, or needles—also seem to emanate from the nucleus, but they tend to be narrow and more sharply-defined than fans (Fig. 2). As with fans, jets can be stable and long-lived, lasting for months. However, they can also be extremely dynamic, changing their appearance or direction on timescales as short as hours. Jets have been detected individually or in groups, and have no preferred orientation. Although both fans and jets are primarily radial, they can both show curvature at increasing distances from the nucleus.

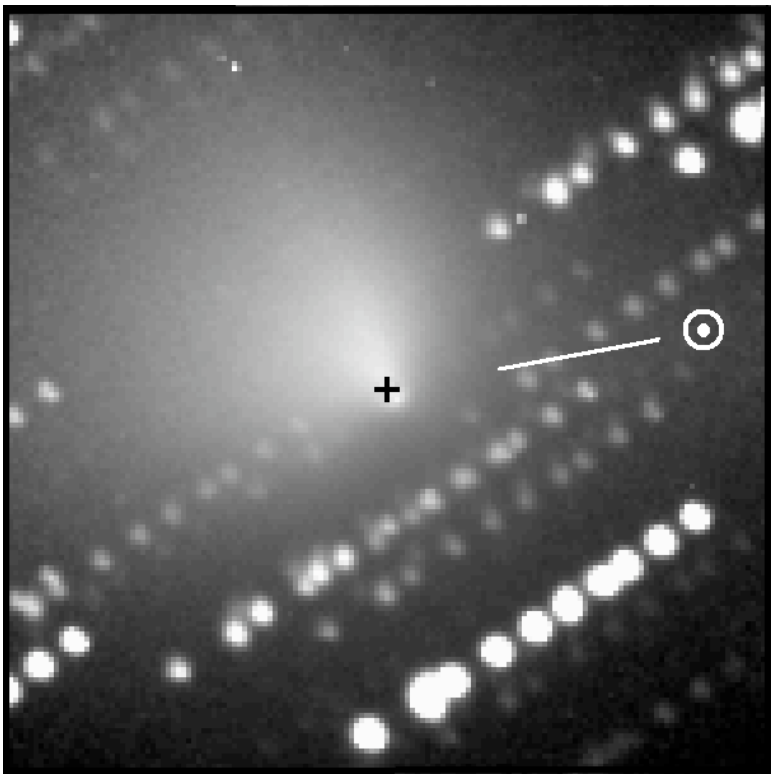

Fig. 1. Image of comet 81P/Wild 2 showing a fan-shaped structure extending perpendicular to the comet's orbital plane. The Earth is within 1° of the orbital plane, which is defined by the comet-Sun line. The coma has been enhanced by division of a $1/\rho$ profile and the "+" marks the optocenter.

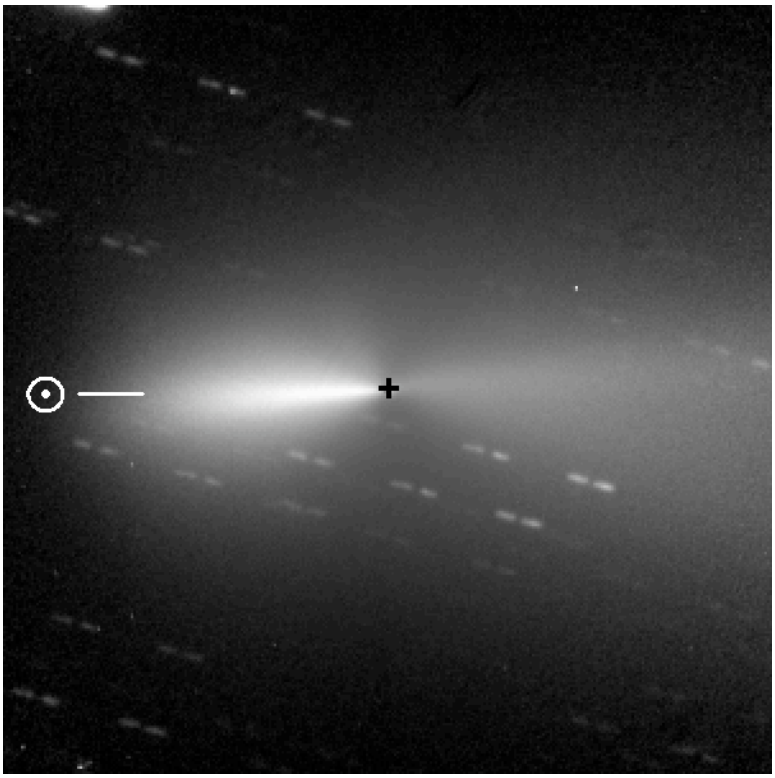

Fig. 2. Image of comet 19P/Borrelly showing the highly collimated sunward jet. The coma has been enhanced by division of a $1/\rho$ profile and the "+" marks the optocenter.

Arcs, Halos, Shells, Envelopes and Spirals. These are features that are primarily azimuthal in form, wrapping around the nucleus in partial arcs or full spirals (Fig. 3). They can be diffuse or have sharply defined edges. Often, multiple "layers" are seen, with a series of successively larger nested shells. The presence of multiple shell groups can also produce very complex morphology, with criss-crossing features and different expansion rates.

Corkscrews and Helices. Somewhat of a hybrid, corkscrews represent a combination of radial and azimuthal structure (Fig. 4). As their name implies, they have the characteristics of a corkscrew viewed from the side, zig-zagging back and forth as the distance from the nucleus increases.

Temporal and Periodic Variations. Though not a type of feature, it is worth noting that temporal variations provide a powerful tool for interpretation of features. Although a single image contains temporal information, in that material at larger distances was emitted earlier, the information is limited and assumptions about motion and change must often be made. On the other hand, a sequence of images can strengthen and clarify the interpretation and allow measurements of outflow rates and other physical properties. Sequences that show periodicity (especially those that have good phase coverage) are especially useful, because they can represent the activity throughout a full rotation cycle.

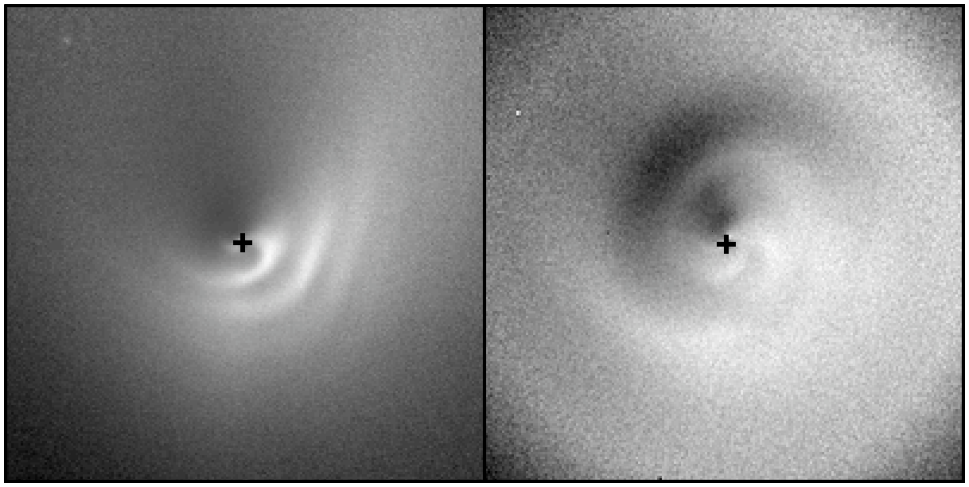

Fig. 3. Images of comet C/1995 O_1 (Hale-Bopp) showing the arcs and spirals in the coma. The left panel shows a dust image, enhanced by division of a $1/\rho$ profile to show partial arcs nested at different distances. The right panel shows a CN image that has been enhanced by division of an azimuthally averaged profile to show complete spirals extending all the way around the coma. The "+" denotes the optocenter in each case. The images were obtained at 2.75 UT (CN) and 2.88 UT (dust) on 29 March 1997.

There are definite relationships between the different types of features listed above. In fact, fans, jets, arcs, and corkscrews may be the same physical entity, taking on different appearances depending on the particular viewing geometry, observing conditions and temporal evolution. These relationships can be exploited for the interpretation and analysis of the coma, as discussed in more detail in Section 4.

Arclets and Wings. Recently, fortuitous circumstances have allowed several cometary splitting events to be extensively observed. Early in some of these events, and usually seen in conjunction with an outburst, there are unusual arclets or wings detected in the coma. These features, which have lifetimes of a few days, have been found in at least four comets around the time of splitting events (Harris et al., 1997; Farnham et al., 2001; Boehnhardt, 2004; Jehin et al., 2002; Hadamcik and Levasseur-Regourd, 2003; Lara et al., 2007). Arclet features, like that illustrated in Fig. 5, are observed in the gap between two nucleus fragments. These structures, which tend to be seen in images of the gas coma, have been interpreted as hydrodynamic shocks that form in the stagnation region between two emission sources (e.g., Rodionov et al., 1998). Comet C/1999 S_4 (LINEAR) exhibited yet another type of feature, with wing-shaped extensions to the sides of the nucleus (Fig. 6). In images processed with an edge-finding technique, these wings initially appear similar to the arclets, but with a more subtle enhancement, they are revealed to be lobes centered along the comet-Sun line. The axisymmetric nature of this structure and the fact that the leading edge appears to converge on the nucleus, suggests that it is rotationally generated. With the spin axis near the plane of the sky the jet will flip from one side to another during a rotation, producing the axisymmetric morphology. This scenario is supported by the appearance of a narrow jet along the edge of the envelope in one image (Fig. 6 inset). It is clear that these features are uniquely associated with the fragmentation process, and their presence could be an indicator of a nucleus splitting, even if a fragment is not detected. Additional details regarding split

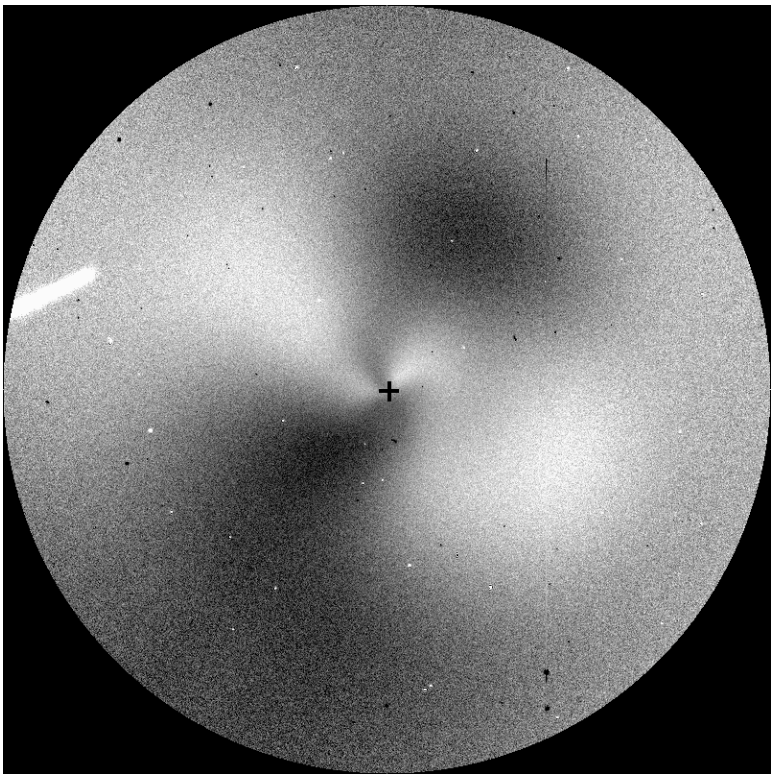

Fig. 4. Image of comet C/2004 Q_2 (Machholz) showing corkscrew-shaped features in the coma. The image was obtained with a CN filter and has been enhanced by division of an azimuthally averaged profile. The "+" denotes the optocenter.

nuclei are discussed elsewhere in this volume (Fernández, 2008).

Transient and Spontaneous Features. There are many different types of features that are produced in outbursts and other transient events (Hughes, 1991). Because these are not periodic, they do not necessarily fall into the same classes as those described above, nor do they necessarily have any common relations between themselves. Examples of these features include the "fried egg" appearance of comet 17P/Holmes in 2007 (e.g., Montalto et al., 2008; Moreno et al., 2008), the varying directions and intensities of the multiple outbursts observed in comet 9P/Tempel 1 during the approach of Deep Impact (Farnham et al., 2007b) and the small, rapidly changing filament "loop" seen in the Deep Space 1 images of comet 19P/Borrelly (discussed in Section 6.1; Boice et al., 2000; Soderblom et al., 2004).

Large-Scale Structures. Comets exhibit other types of features that can all be classified as large-scale structure: Dust tails and plasma tails tend to lie in the anti-sunward direction (Brandt, 1982); anti-tails may be visible directed toward the sun if observing conditions are right (Sekanina, 1974); neck-line structures can be seen where orbital mechanics conspire to reconcentrate dust that was emitted earlier in the orbit (Pansecchi et al., 1987); dust trails spread out along the comet's orbit and may become very extensive (Sykes, 1988; Reach et al., 2007); and asymmetries and shapes are seen in extreme ultraviolet and X-ray observations of the coma (Krasnopolsky et al., 2004). Although these structures are indeed dependent on

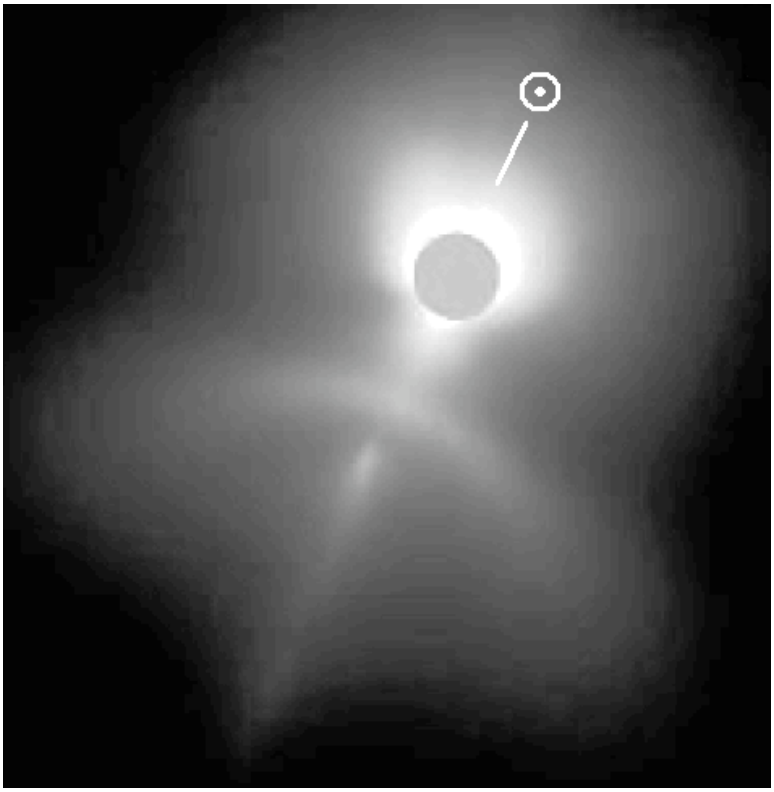

Fig. 5. Image of comet C/1996 B_2 (Hyakutake) during a fragmentation event (from Harris et al. (1997). Reprinted with permission from AAAS.) The nucleus is hidden under the grey circle and a fragment is located along the comet-Sun line, just below the center of the frame. An arclet is located in the gap between the nucleus and the fragment, bending away from the Sun. The image was obtained with a CN filter and contains both CN and its underlying continuum.

the properties of the nucleus for their existence, their general appearances are dominated by the effects of the solar environment, so they will not be addressed here in any detail.

2.2 Image Enhancement

In any extensive discussion of coma features, the issue of image enhancements will inevitably arise. It is the nature of cometary comae that the ambient coma and the various features can comingle, reducing the contrast and confusing the appearance of basic structures. Image enhancements provide a tool for at least partially undoing these problems, to improve the contrast and make it easier to identify and interpret the structures that are present. These techniques have become nearly ubiquitous in comet observations, because they can be simple to use and have the potential to reveal important and useful information.

A large variety of image processing techniques is available (e.g., Schwarz et al., 1989; Larson and Slaughter, 1992; Schleicher and Farnham, 2004; Samarasinha et al., 2006, and references therein). Although they differ in the details of how they work, the goal is usually to remove

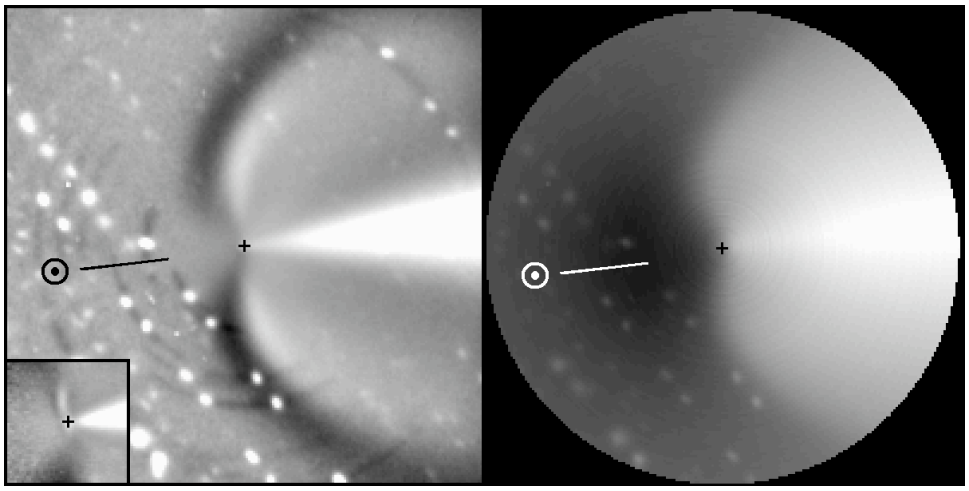

Fig. 6. Image of comet C/1999 S_4 (LINEAR) during an fragmentation/outburst event. The left panel has been enhanced by division of a 45° rotationally averaged profile to show the wings converging on the nucleus. The right panel has been enhanced by division of an azimuthally averaged profile to show that the features are actually axisymmetric lobes centered on the comet-Sun line. The inset shows the coma from the following night, when a narrow jet was visible along the leading edge of the wings. The "+" marks the optocenter in each case.

the bright central condensation at the nucleus, leaving behind a more uniform background that highlights the more subtle variations. Once the features have been identified in enhanced images, it is usually possible to return to the original image and find the feature there simply by using targeted display parameters.

The application of image enhancement techniques also has hazards, which are more fully discussed in the manuscripts cited above. Processing the data unavoidably alters the image and has the potential to introduce artifacts that can be misinterpreted as features, while improper centering or normalization can also introduce false features that may be interpreted as real. Because the different techniques affect the image in different ways, it is a good idea to experiment with several, applying them to the same image to help in evaluating whether features are real or not. Another hazard is in the interpretation of the features after the images have been enhanced. Users should be aware that the appearance of the features can be fundamentally different in the enhanced version. A simple example arises when an edge-finding routine (e.g., shift differencing or a Laplace filter) is applied to a fan-shaped coma. The edge-finder will highlight the sides of the fan, while flattening the regions inside and outside. Thus, the result is a processed image that reveals what appears to be two narrow jets rather than a single broad fan (Samarasinha et al., 2006). These hazards argue for always returning to the original image to evaluate the features that are revealed. Other techniques, such as following the systematic shape of the coma isophotes can also be used to evaluate the existence of features.

Finally, it should be stressed that models should not be constrained using only the enhanced data. Modeling the two narrow jets in the example gives a dramatically different result from the fan model that should be used. Instead, the original coma should be used for the

modeling, and if comparisons to the enhanced image are needed, then the modeled image should be processed in the same way as the observed images.

3 Feature Formation Mechanisms

In order to use morphology to extract information about the coma, we need to understand the mechanisms that act to produce the features. The interpretation of structures in cometary comae generally falls into two groups: physical variations in the coma produced by collimated jets and nonisotropic emission, and hydrodynamic interactions that produce density enhancements as a result of topography and shocks. We now address these mechanisms and summarize how they produce the observed morphology.

3.1 Collimated Jets

The fountain model of the cometary coma was originally introduced by Eddington (1910) to explain a series of envelopes observed in the sunward direction of comet Morehouse. In the fountain model scenario, material ejected from the nucleus is pushed away from the Sun by solar radiation pressure or the solar wind, imparting a parabolic trajectory on each individual dust grain. Under these conditions, the ensemble of all particles forms a parabolic envelope, with the focus at the nucleus, the apex in the sunward direction, and the size and shape of the envelope governed by the particle size distribution and the emission velocity of the dust. Since its introduction, the simple fountain concept has been expanded dramatically to include many other processes.

The contemporary model for coma morphology, introduced by Sekanina (1987a), invokes anisotropic emission to explain the presence of features. In this model (hereafter referred to as the collimated jet model) isolated active regions on the nucleus emit gas and dust that flow out into space, producing spatial variations in the coma. Because the material in different jets can come from different sources, this mechanism provides a natural explanation for the difference in the properties (density, outflow velocity, particle sizes, etc.) that are often distinguishable in different features and in the ambient coma. The active areas in this scenario can be attributed to regions of higher gas production, possibly due to inhomogeneities in the composition of the ices driving the activity, or they may represent true vents or cracks in an otherwise impermeable mantle. (Evidence for mantle formation on comets is discussed in Section 3.1.1.)

All the various feature classes have natural explanations in the collimated jet model, with some features explained in multiple ways. Narrow jets are highly collimated flows, which produce a high-density region expanding radially away from the nucleus. (A discussion of collimation is presented in Section 3.1.2). In an analogous manner, fans may be produced by larger active areas, sources with a wide opening angle, or as the superposition of multiple

narrow jets. For an active region near the equator of a rotating nucleus, the radial outflow will form an archimedean spiral, which can take on the appearance of several different structures depending on the particular observing conditions. When viewed from above or below, observations of the near nucleus region will show a radial jet, intermediate-scale observations may show a straight jet that curves at its end, and large-scale observations will show a classic spiral or nested shell structures. When viewed edge-on, a pair of linear jets may be seen in opposite directions. In between these viewing extremes, the arms of the spiral may appear as parabolic or elliptically-shaped envelopes.

A variation on this configuration arises when the active region is at a high latitude, so that it sweeps out a cone centered on the comet's spin axis[1] , as the nucleus rotates. In this case, a modified archimedean spiral is formed along the sides of the cone. When observed from within the cone, complete spirals may be seen, though they will be distorted if the observer is close to the edge of the cone. From outside the cone, corkscrews or helices may be discerned if the rotation is slow compared to the emission velocity. For a fast rotation, the individual spirals merge together to fill in the walls of the cone to form a fan-shaped feature. In this configuration, the planetary nebula effect may also manifest itself, so that the edges of the cone appear as radial rays or spikes. Because the cone is centered on the comet's spin axis, the rays are frequently found in pairs with the projected axis centered between them. This represents a special case for determining rotational properties as discussed in Section 4.

Features produced by the collimated jet model are also affected by other, more complex factors. For example, radiation pressure acts to distort the dust features, affecting the basic appearance that might be expected from simple outflow models. Because the effects of radiation pressure are more efficient for smaller dust particles, including them in the analysis can provide information about the grain sizes. Other effects complicating feature interpretation include jet activity that turns on and off over the course of a rotation (e.g., as the source rotates in and out of sunlight). In this case, only partial arcs or segments of a corkscrew will be formed. Similarly, only one edge of a cone may be visible, which can lead to miscalculation of the pole orientation if multiple half-cones are produced. Diffusion of the dust and gas in the jets and the resolution of the observations also both play a significant factor in the appearance of the coma. Even highly collimated jets experience lateral diffusion due to the random velocity variations in the flow, and this diffusion causes the spirals to disperse outward into the intervening gaps between the arms. With a high degree of diffusion, the spread may ultimately reach the point where the outer arms blur together until they are indistinguishable from each other (Sekanina, 1991c). Alternatively, observations with insufficient resolution may not be able to separate the individual spirals at all, in which case the coma will exhibit a round or elliptical shape.

This result highlights the fact that a lack of observed features doesn't necessarily mean that the coma doesn't have structure or that the nucleus does not have discrete sources. In fact, the presence or absence of features is strongly dependent on many factors, including the

[1] The terms "spin axis" and "rotation pole" are used throughout to refer to the instantaneous spin state of the nucleus. For simple rotation, this also corresponds to the angular momentum vector.

viewing geometry, the coma brightness, the comet's proximity to the Earth, etc. Features may be faint or have a low contrast against the rest of the coma (even with the use of enhancements), making them difficult to detect. Because most comets never approach the Earth, features often remain undetected, hidden in the inner coma or unresolved due to atmospheric seeing. For example, all of the comets imaged in situ by spacecraft (1P/Halley, 19P/Borrelly, 81P/Wild 2 and 9P/Tempel 1) have displayed broad fans and jets in ground-based studies, but have shown many more intricate features in the approach and encounter images. Similarly, Hubble Space Telescope (HST) observations often reveal features that are not otherwise seen from the ground, and comets that do approach to the Earth (e.g., 2P/Encke, C/1996 B_2 (Hyakutake), 73P/Schwassmann-Wachmann 3) reveal well-defined structures when they are near, but appear featureless when they are more distant. This suggests that features probably exist at various different scales in most comae, but are simply unresolved with improper observing conditions. Geometric effects and observing conditions also act to hide features. Projection effects can place a jet or fan in the anti-solar direction where it is mistaken for a tail; an observation along the centerline of a cone may be interpreted as a round, featureless coma; poor seeing can smear out features, while improper guiding can act to mimic them; and image processing can remove or alter structures, or introduce artifacts that can be misinterpreted as real structure.

3.1.1 Evidence for Mantles and Active Areas on Comets

The collimated jet interpretation for coma features is dependent on the existence of discrete outgassing areas on the surface. This requires that the gas emission must be reduced, or shut off altogether, over large portions of the nucleus, implying that an inactive mantle of some type covers the nuclei of most comets (e.g., Mendis and Brin, 1977; Brin and Mendis, 1979). There are suggestions that the mantle consists of a cohesive layer, bonded by organics, that seals the surface (Smoluchowski, 1989; Seiferlin et al., 1995), but this concept has evolved into a more regolith-like layer that may be quite thin with low tensile strength.

There is a significant amount of observational evidence for inactive surfaces and active areas. First is the small active fraction of most comets. Measurements of the water production rate (or as a proxy, the OH production) give an estimate of the surface area that must be sublimating, and using the total surface area from measurements of the size of the nucleus, the active fraction can be determined. For most comets, only a few percent of the comet's surface is active (A'Hearn et al., 1995; Tancredi et al., 2006, among others). Second, seasonal effects are common, with many comets being more active before perihelion than after, or vice versa (e.g., Campins et al., 1982; Sekanina, 1988a,b; A'Hearn et al., 1995). These asymmetric production rates do not scale directly with heliocentric distance and can only be explained by inherent differences in the activity across the surface. Third, the commonly accepted explanation for nongravitational forces is based on nonisotropic emission. Although this constraint is not necessarily required (Sekanina, 1984), detailed analyses of particular comets have usually found that isolated active areas produce the best result for modeling the perturbations to the comet's motions (e.g., Sekanina, 1984; Rickman et al., 1991; Krolikowska et al., 1998; Yeomans et al., 2005). Fourth, when comets fragment or split, the event

is often accompanied by an outburst of activity. The production rates can temporarily rise to several times the ambient level and strong jets may be seen, suggesting that part of the inactive surface has been removed and fresh material has been exposed to the Sun (Boehnhardt, 2002). Finally, models of the dust trails that produce meteor showers often work best when the dust is emitted from narrow jets rather than isotropically (Welch, 2003).

Observations of the comets visited by spacecraft provide additional support for mantles on these comets. The Deep Space 1 (DS1) Miniature Integrated Camera and Spectrometer (MICAS) measurements of 19P/Borrelly show that there is no evidence of water ice on the surface and that the temperature is around 300 K (Boice et al., 2000). Similarly, temperature maps created from the DI High Resolution Instrument Infrared Spectrometer (HRI-IR) show surfaces on 9P/Tempel 1 between 290 and 340 K. These temperatures are too hot for ices to exist for long, confirming that there must be a hot, dry layer covering the surface.

DI images of the coma of 9P/Tempel 1 also show strong evidence for active areas on the surface. Images created from IR spectral scans, also reveal nonisotropic emission of H_2O and CO_2 (Fig. 7; Feaga et al. 2007), where isolated sources produce features that are many times brighter than other regions of the coma. These images clearly show that the nucleus is not uniformly active in gas production. Furthermore, the nature of the coma structures and locations of the sources, as well as the fact that they are not the same in the H_2O and CO_2 images, suggests that the variations in activity across the surface cannot be simply attributed to the illumination conditions. Although the local solar insolation undoubtedly plays a role in modifying the production rates, active and inactive regions, as well as inhomogeneities in the nucleus composition must play a primary role in producing the observed morphology.

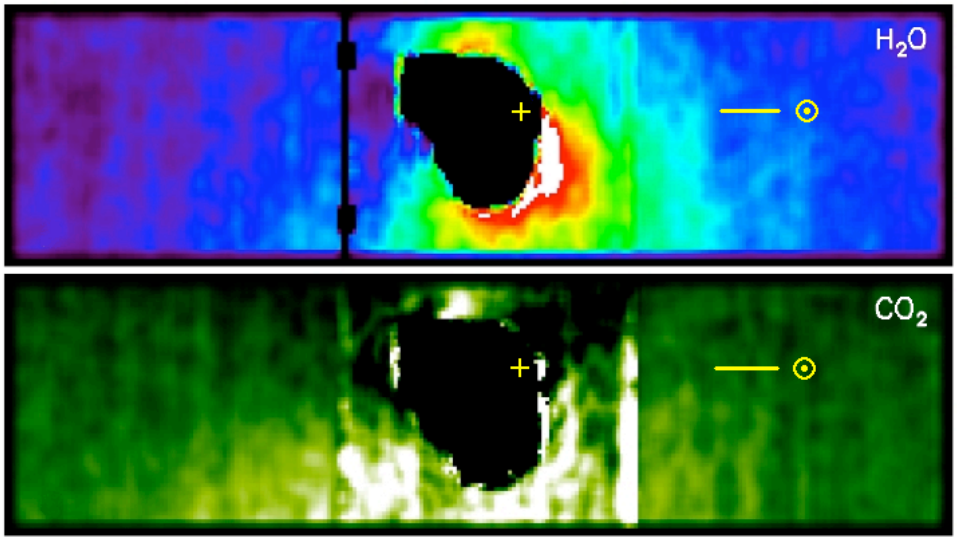

Fig. 7. Deep Impact Infrared Spectrograph "images" of 9P/Tempel 1 (Feaga et al., 2007). The top panel shows the H_2O structure in the coma, and the bottom panel shows the CO_2 coma. The yellow "+" denotes the approximate location of the sub-solar point on the nucleus, which is blacked out. The vertical discontinuities to either side of the nucleus are artifacts produced by the anti-saturation filter on the instrument.

The IR scans, along with narrowband imaging from the DI cameras, do reveal water ice on the surface, though only in a few small patches and in very small amounts (Sunshine et al., 2006). Because of the high temperatures noted above, these water ice patches must be transient, and are probably recondensation from residual emission that continued during the night (the patches are located on a portion of the nucleus that just rotated into sunlight). Associated with these patches are small (∼10 m), dense dust jets that appear to project directly from the surface adjacent to the water ice (Fig. 8; Farnham et al. 2007b). The correlation between these characteristics suggests that the jets arise from small, active vents, driven by the sublimation of sub-surface ices. Furthermore, the images of the H_2O and CO_2 comae (Fig. 7), both show a minor peak in emission just above this location on the nucleus, indicating that it is truly an isolated source of emission. The presence of CO_2 emission means that the vent could have remained active well after sunset the previous rotation, aiding in the ejection of water that recondensed on the surface.

The Deep Impact experiment at 9P/Tempel 1 provides especially strong evidence for an inactive layer. Results from the impact indicate that the nucleus has a low tensile strength. The crater ejecta had a high dust-to-gas ratio, with small dust grains and nearly pure water ice (A'Hearn et al., 2005). More detailed analysis indicates that, although the surface is essentially devoid of volatiles, fresh, unaltered water ice is reached at a depth of only about a meter (Sunshine et al., 2007). This puts a tight constraint on the surface properties of 9P/Tempel 1, revealing a thin, regolith-like covering that is highly porous. A low thermal inertia effectively insulates the underlying ices from the hot surface.

Theoretical models and laboratory experiments have been used to explore the evolution of the comet's surface over time (Gruen et al., 1991; Kührt and Keller, 1994; de Sanctis et al., 1999; Klinger, 1999, and references therein). Both theoretical and laboratory simulations agree that the production of a depleted surface layer is essentially an inevitable result in virtually all comets (Ibadinov, 1989; Thiel et al., 1989, 1991; Orosei et al., 1995; de Sanctis et al., 2003; Prialnik et al., 2004; Laufer et al., 2005). Whipple (1978) proposed the basic scenario that as a nucleus approaches the Sun, solar insolation vaporizes the ices, which entrain the surface dust and pull it off the nucleus. In a highly active comet, all of the overlaying dust may be blown off the surface, but for most comets, some of the dust will remain behind, building up over time to form the insulating mantle. As the gas flow is restricted (as little as 1 cm of mantle can reduce emission by a factor of 10 (Rickman, 1991; Ibadinov, 1999; Ibadinov and Rahmonov, 2002; Skorov et al., 2002)), even more dust will remain behind, further cutting of the activity. This is a self-limiting process, because eventually the layer gets thick enough to shut off activity altogether.

There are other processes that can also contribute to mantle formation. The first is the ballistic trajectory of slow-moving dust particles. Low-velocity grains emitted from active regions can migrate to other spots (even on the night side) and settle back onto the surface (e.g, Kitamura, 1986). Thus, a jet in one spot may be strong enough to keep from choking itself off, but the ejected material can contribute to mantle formation elsewhere. Cosmic rays also act to create a devolatilized layer (e.g., Jewitt, 2004b). This process acts continuously, even

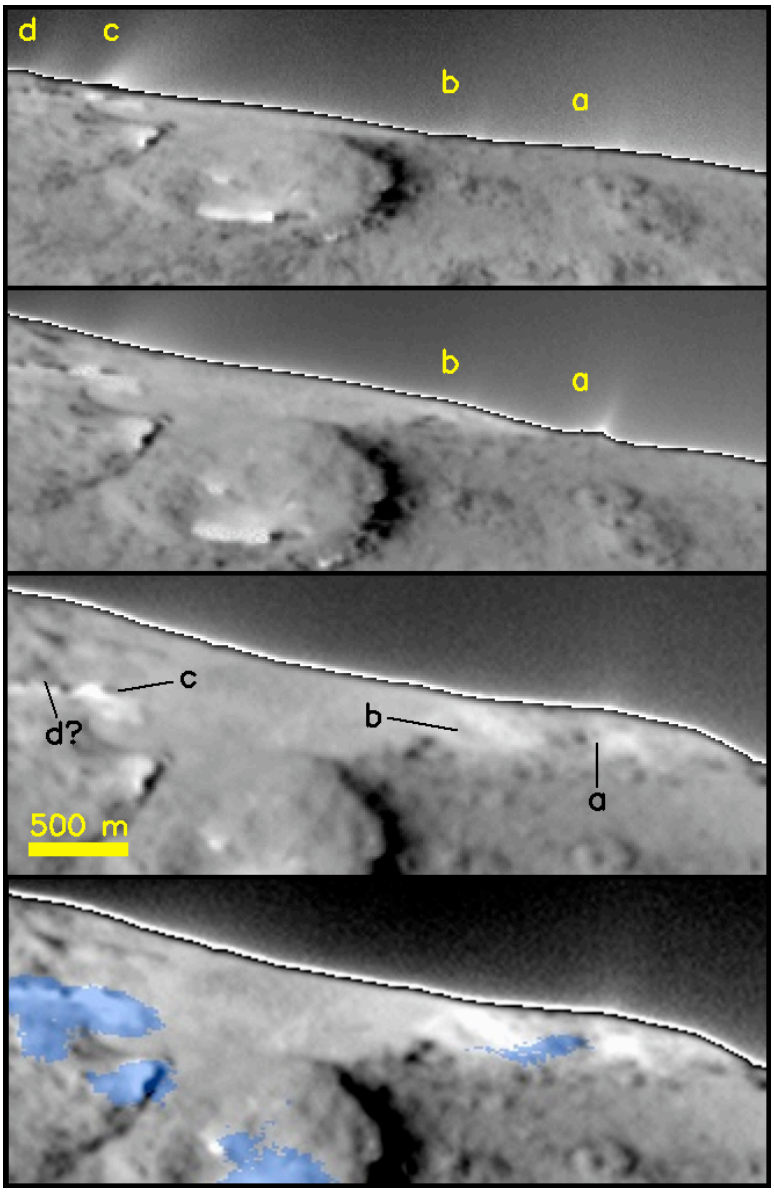

Fig. 8. Deep Impact images showing the small surface jets on the limb of comet 9P/Tempel 1 (Farnham et al., 2007b). As the spacecraft passed under the nucleus, the jets appeared to cross over the horizon. The approximate sources of the jets are marked in the third panel, and for comparison, the patches of surface ice are shown in blue in the bottom panel.

when a comet is not active, processing the upper layers of the nucleus through vaporization and spallation (Schulz et al., 2005). Although this is a slow process, it acts on the surface all comets, which explains why even dynamically new comets can exhibit discrete outgassing regions. Highly volatile materials concentrated near the surface may also be a by-product of this process (Johnson et al., 1987; Smoluchowski, 1989), which may contribute to dynamically new comets showing extreme activity early on, and then flattening out as they get closer to the sun.

In general, a comet's decrease in activity is thought to be due to the overlying mantle growing dense enough to be impermeable to the gas flow (e.g., Whipple, 1978; Rickman, 1991; Ibadinov, 1999). However, the DI results show that the surface of Tempel 1 has a highly porous nature (e.g., Richardson et al., 2007), which should easily allow gas to escape (e.g., the friable sponge model introduced by Horanyi et al. (1984)). Furthermore, Prialnik et al. (1993) have used simulations to suggest that the flow through the matrix capillaries might even act to straighten the pores and keep them from sealing themselves off. These results suggest that another factor—the thermal properties of this porous matrix—could play a significant role in impeding the comet's activity. The thermal conductivity at the surface is low enough that a meter of material can effectively insulate the internal ices from the 300 K temperatures at the surface (Groussin et al., 2007), so rather than trapping gas under the surface, the role of the mantle may be more important as a means of limiting the amount of ice that sublimates into gas (Thiel et al., 1989).

If mantle formation is a ubiquitous process on comets, how is it that comets exhibit significant amounts of activity? The answer to this question is not fully understood, but a number of possibilities have been proposed. First, some of the sun's energy undoubtedly penetrates the mantle to sublimate the subsurface ices, and the gas that is produced can easily percolate out through the mantle. Vents or highly active areas may be strong enough to keep themselves cleared of material (thus producing long-term coma features that can be seen over multiple apparitions). Spacecraft observations have also revealed interesting surface topographies on 19P/Borrelly, 81P/Wild 2 and 9P/Tempel 1, that suggest a possible solution. All three comets show steep cliffs or "mesas", with evidence that jet and fan activity arises from the sides of these structures (Boice et al., 2000; Sekanina et al., 2004; Farnham et al., 2007b). It is possible that activity arises from these nearly vertical faces and as the ice sublimates, it undercuts the surface mantle. Residual dust that is not lifted off the surface falls to the bottom of the cliff, leaving the fresh ices exposed. Additional evidence for undercutting of the surface comes from the detection of intricate arches and overhangs on comet 81P/Wild 2 (Brownlee et al., 2004b). These must have been formed by the erosion of underlying material, which left the delicate structures suspended in space. Other features seen on both 81P/Wild 2 and 9P/Tempel 1 appear to be cracks (Brownlee et al., 2004b; Thomas et al., 2007) that could result from thermal stresses across the surface (Tauber and Kührt, 1987; Jenniskens and Blake, 1996). This type of crack would reveal fresh subsurface material, providing a mechanism for creating new regions of persistent activity.

3.1.2 Collimation of Cometary Emission

Another issue that must be addressed in regards to the collimated jet model is the comet's ability to collimate the outflowing material into well-defined jets. The basic principles of gasdynamics show that the random thermal motions in a stream of gas will cause a stream of gas to rapidly diffuse laterally when it issues into a vacuum environment. In a collimated flow, the radial velocity of the particles is much larger than the random thermal motions, which allows the stream to retain some degree of its general structure. When the flow expands beyond the collisional zone, it enters a free-flow regime, and whatever structure that remains

will be preserved to very large distances (until it is perturbed or destroyed by the solar environment). The gas flow is most susceptible to the random thermal motions near the comet's surface where the density and temperature are both high. The effect falls off with distance, as the expanding flow rapidly cools and disperses. The dust in a typical comet, on the other hand, can decouple from the gas at a few nuclear radii, making it much easier to collimate than the gas.

A number of different collimation mechanisms have been proposed. As will be discussed in Section 3.2, the topography of the surface can affect the gasdynamic flows, and this was one of the earliest mechanisms proposed for collimating jets. Models have shown that trenches, craters and facets (including the angle where a cliff face meets the horizontal surface) can produce a "lens effect", where the insolation from the sun is reflected and focused by the opposing surfaces (Colwell and Jakosky, 1987; Colwell et al., 1990; Keller et al., 1994; Ivanova and Shulman, 2002; Huebner, 2003; Keller et al., 2004). Due to this self-radiation, the bottom and sides of the topographic feature to heat up, increasing the sublimation rate. The interaction of the gas flowing from these offsetting surfaces also acts to focus the outflowing gas, producing a collimated stream. The lens effect is a self-propagating mechanism, because the increased sublimation that arises from the focusing also causes the crater to deepen, intensifying the effect even further (though at some point, self-shadowing will limit the effect). This reflective heating has been invoked as the mechanism for explaining the details in the temperature map of the surface of comet 9P/Tempel 1 (Groussin et al., 2007, and private communication).

The mechanism usually invoked for collimating flows is the venturi effect, which may act alone or in combination with the cavities or chambers below the surface. The venturi effect—the supersonic acceleration of a fluid passing through a nozzle—may focus a flow enough for it to retain its jet structure. The focusing effect is especially pronounced for the dust, which is more likely to remain collimated, even if the gas expands laterally. The venturi effect may also be produced in capillary "tubes" in the mantle, with each tube acting as a miniature nozzle (Skorov and Rickman, 1995). If a number of these tubes are distributed around a region on the surface (e.g., an active area) then the superposition of the individual tubes will contribute to what is observed as a single jet. Furthermore, the lateral diffusion of the sources around the perimeter of the active area have a component that converges inward. This inward flow generates a ram pressure that will reduce the lateral diffusion of the sources near the center and increase the degree of collimation of the overall jet. Using laboratory experiments, Thiel et al. (1991) showed that gas percolating through a matrix surface does seem to induce collimation in the outflowing dust, which supports the possibility that this may be one means of producing jets.

More recently, the role of subsurface cavities that vent through passages to the surface has begun to be explored in detail (e.g., Yelle et al., 2004; Davidsson, 2007). These cavities, which have been likened to geysers, show promise as a mechanism for explaining not only jets, but also outburst events. In this scenario, pockets of gas form beneath the surface and the venting gases are collimated by the venturi effect as they flow through the passage to the surface. Typically, a vent with a length-to-width ratio of a few can produce a highly

collimated jet.

Unfortunately, although their pros and cons have been debated and simple models have been tested, none of these mechanisms has yet been extensively evaluated to determine whether any of them are sufficient for producing the types of jets seen in comets, which means that there is currently no widely accepted mechanism for collimating jets. True tests for proving the potential of any of the proposed processes will require detailed hydrodynamic models that specifically address the physics of collimation, flows through porous surfaces, etc. However, the fact that we don't fully understand the complexities of collimating jets does not mean that they cannot exist, and in fact, there is a wealth of observational evidence in support of collimation.

The strongest proof for collimated features comes from continuum images of comet 19P/Borrelly. Both ground-based and DS1 observations clearly reveal a narrow jet, with a width of about 20°-30° (Fig. 2) and a surface brightness (in the ground-based images) at least three times higher than the coma 90° away (Farnham and Cochran, 2002). The same fundamental structure is observed at a broad range of spatial scales and observation times. In the close approach images, it extends from the limb of the nucleus (where it is lost against the brighter surface) to the edge of the frame at ∼100 km (Thomas et al., 2001; Soderblom et al., 2002); at intermediate distances, from hundreds to thousands of kilometers, it is seen during the approach phase of DS1 (Thomas et al., 2001) and in high-resolution HST observations (Lamy et al., 1998; Weaver et al., 2003); and at large scales—out to hundreds of thousands of kilometers—it is detected in ground-based images (Fulle et al., 1997; Farnham and Cochran, 2002; Samarasinha and Mueller, 2002; Szabó et al., 2002; Schleicher et al., 2003; Ho et al., 2004).

On recent apparitions, the structure of the jet remains essentially unchanged throughout the entire time that the northern hemisphere is in sunlight (for more details, see Section 6.1). It is also highly reproducible from one apparition to another (Fulle et al., 1997; Farnham and Cochran, 2002). During the DS1 encounter images, the viewing geometry changed by about 40° with the biggest change taking place in the last few minutes (e.g., rotation of the comet can be neglected), and in the months around perihelion, the ground-based viewing geometry changed by ∼70°, yet the jet always had the same characteristics. In order to present this same appearance regardless of time, rotational phase, or viewing direction, the jet must be a narrow cone, which suggests that it is an axisymmetric, highly collimated flow of dust.

The issue of collimated features is more confusing for the gas than for the dust. For example, even though it has a highly collimated dust jet, comet 19P/Borrelly shows little collimation of the gas that it is emitting (at least at large spatial scales—the DS1 images did not isolate gas species). Images of the gas coma show a hemispheric asymmetry, with the sunward side 2–3 times brighter than the anti-sunward side, but no sharply defined features are seen (Szabó et al., 2002; Schleicher et al., 2003). This seems to support the conjecture that both the gas and dust are originally collimated, but decouple very close to the nucleus, allowing the gas to expand laterally without affecting the dust. On the other hand, well-defined gas structures have been observed in other comets, starting with the CN and C_2 jets in the

coma of comet 1P/Halley (A'Hearn et al., 1986a,b). Since then, a wide range of structures have been observed in images of various gas species, including shells, fans, jets, and even helices (e.g., Schlosser et al., 1986; Cosmovici et al., 1988; Suzuki et al., 1990; Spinrad, 1991; Boehnhardt and Birkle, 1994; Mikuz, 1994; Eberhardy et al., 2000; Lederer and Campins, 2002; Veal et al., 2000; Schulz, 2002; Szabó et al., 2002; Lara et al., 2004; Farnham et al., 2007a; Lin et al., 2007). In some comets, the gas features are coincident with the dust, while in others there is no correlation. Other comets have well-defined gas features, even though their dust structures are minimal or completely absent. To complicate the issue even further, CN and C_2 are daughter or granddaughter species that are presumably emitted isotropically from a parent molecule. This affects the collimation of the flow and the shape of the features, especially if the dissociation velocity is near the parent gas outflow velocity.

Because of the dilemma in maintaining collimation of the gas, it has been suggested that these features are not truly gas flows arising from the nucleus, but instead are actually streams of tiny dust grains (e.g., the "CHON particles" detected in comet 1P/Halley (Kissel et al., 1986)) that release various gases as they disintegrate (Combi, 1987; Klavetter and A'Hearn, 1994). If this is the case, the collimation process for dust grains can be invoked to explain the well-defined structure, with the gas being produced as a secondary product further out in the coma. This is discussed more fully in Section 4.

There is one set of observations that may actually show collimation of gas emission, however. (Whether it is coincidence or not, the observations come from the only comet where gas structures have been observed in association with a resolved nucleus.) The H_2O and CO_2 images of comet 9P/Tempel 1, produced from spatial scans with the Deep Impact IR spectrometer, show gas structures that seem to retain some degree of collimation (Fig. 7). The H_2O image reveals several sources, the most intense of which is near the sub-solar point at the right of the nucleus, with a smaller source $\sim$90° away toward the North (at the top of the image). The largest jet appears to remain partly collimated out to several nuclear radii, leaving a low-density gap between it and the northern source. This gap exists even at the limb, where the lateral surface flows are expected to be strongest. There is also a CO_2 jet to the southeast (where there is another deficiency of H_2O) that appears to remain partly collimated to the edge of the field of view. This is especially interesting because it adjoins the low density region on the anti-sunward side of the nucleus. It is possible that these structures are the result of the gas flows interacting with topography (which should be investigated more fully), but it could also be the first evidence for true collimation of cometary gas emission.

3.2 Hydrodynamic Interactions

Though the collimated jet models have dominated the analysis of coma morphology, more recent models have been developed to incorporate more sophisticated gasdynamic physics. These hydrodynamic and physicochemical models have been developed to study the interactions of gaseous and dusty-gas flows in the near nucleus region, to determine how they

can affect, among other things, the coma morphology. In these scenarios, the observed coma features are a produced, not only by variations in the activity across the surface, but also by interactions of different gas and dust flows. These interactions can produce shocks or high density regions that can be interpreted as jets. Reviews (both basic and extensive) covering the intricacies of the physical interactions between the gas, dust and nucleus are available (e.g., A'Hearn and Festou, 1990; Keller, 1990; Combi et al., 2004; Crifo et al., 2004; Crifo, 2006), so we only present a brief summary here, with specific reference to their influence on the coma morphology.

Because of the complexity of the physics that must be addressed, this field is effectively still in its infancy, even though it has advanced significantly in the past few years. Generating a complete and accurate hydrodynamic model is extremely difficult, because of the large number of factors that influence the gas and dust flows in the coma. A truly comprehensive model must address: A multidimensional, multicompositional, time-dependent portrayal of gas and dust in several different types of flow regime (collisional, transitional and free-flowing); Dissociation and photochemistry in the coma, which randomizes the flow and changes the properties of the gas; A proper treatment of the boundary layer problems at the surface of the nucleus where the gas flows are not in equilibrium and dust densities are high; The thermal properties of the nucleus, where surface heating imparts energy into gas flows and sublimation and re-condensation add and remove coma material; The activity at the surface, including spatial distributions of the active areas and the temporal changes that occur due to rotation; The effects of topography of the nucleus' surface, at both large and small scales; The thermal interactions of the dust, which heats the gas in the coma; The dynamics and evolution of dust grains in the coma, which are influenced by multiple forces that change as the grains sublimate or fragment; Extended gas emission from sublimation of icy grains in the coma; etc. Some of these factors are more important than others (though which is which is not always obvious until they have actually been compared), and some can be neglected for highly productive comets, weak comets, or comets with a low dust-to-gas ratio. In any case, current hydrodynamic models must make assumptions and simplifications in order to focus on specific aspects of the comet's behavior.

The earliest of these models began with simple one- and two-dimensional studies of a single jet issuing into a vacuum or low-density environment (Wallis, 1982; Gombosi et al., 1985; Vergazov and Krasnobaev, 1985; Kitamura, 1986, 1987). Even these highly simplified models suggested that the random thermal motions in the gas produce a lateral diffusion that dramatically alters the original radial flow of the jet. If the jet issues into a vacuum, then there is nothing to resist the expansion, allowing the flow to wrap almost entirely around the nucleus. On the other hand, if the jet issues into an ambient coma, then as the jet expands, its internal pressure drops until it can be supported by the ambient coma. The interaction of the expanding jet material and the ambient coma can produce a high-density compression region, forming a cone around the central axis of the jet. When seen side-on, the edges of this cone may appear to be a pair of jets, centered on the axis of the original jet.

Later models included temporal variations in the gas flows as applied to rotational modulation and outbursts (e.g. Gombosi and Horanyi, 1986; Combi, 1996), which showed that

shell structures can be produced by modulation of the gas production. Investigations of the interactions between two or more jets (Kitamura, 1990; Crifo et al., 1995) showed that planar shocks result, with a corresponding increase in the density in the interacting region. Similar studies of the dust and gas (e.g. Combi et al., 1997) started to explore how issues such heating from the warm dust grains can produce feedback by introducing an additional source of heating for the gas.

A new generation of more sophisticated models is currently under development to produce a better representation of the dusty-gas dynamics (Crifo and Rodionov, 1997; Gutiérrez et al., 2000, 2001). Using a three-dimensional, time dependent model, these researchers attempt to properly address the flows in the collisional, transition, and free-flow regions, as well as providing better treatment of the boundary layer at the surface of the nucleus. They also use shape models of the nucleus to model the effects of topography and solar illumination. The models have been used to reconfirm and expand on the results of the early studies, as well as to sample different regions of parameter space to determine how they affect the coma.

These models have shown that it is possible to use hydrodynamic processes to reproduce some of the basic types of features seen in the near-nucleus observations. Planar gas shocks seen edge-on may be mistaken for a jet (Crifo et al., 1995). In the same way, very small dust grains can become so entrained in the gas flow that they also exhibit density enhancements along the shocks (e.g., Combi et al., 1997), which can mimic dust jet structure (though larger grains can pass through the shocks unaffected). Rodionov and Crifo (2006) found circumstances where consecutive spiral arcs are produced in the gas coma of a Hale-Bopp-type comet. Another interesting result from these analyses is that, even with homogeneous emission, the effects of large-scale topography can conspire to produce features in the coma. This principle was applied, in conjunction with the nucleus shape model, to generate coma models of comet 1P/Halley (Crifo et al., 2002; Szegö et al., 2002). Results from these simulations produce radial structures similar to those seen in the Giotto and Vega images.

Based on the results obtained for comet 1P/Halley, these authors suggest that homogeneous emission, tempered by solar insolation and surface topography, is sufficient for producing coma morphology, thus challenging the need for invoking isolated active areas to produce coma features (Crifo et al., 2002). When this issue was raised, there were no observations available to prove or disprove the conjecture, but results from the Deep Impact mission now provide an answer. The H_2O and CO_2 observations discussed in Section 3.1.1 (Fig. 7) clearly show that there are active and inactive regions that have no direct correlation with the local illumination conditions. The sub-solar point is a region of low activity, while a number of discrete sources are scattered around the surface. Thus, the only available measurements of gas emission from a resolved nucleus show that isolated active areas do indeed exist and almost certainly contribute to the formation of features in the coma.

3.3 Suitability of the Models

The hydrodynamic and collimated jet models represent very different approaches for learning about a comet's coma. Each has its strengths and limitations, subject to the observational constraints and assumptions that are adopted. Although they are both used to evaluate the structure and features in the coma, they generally focus on separate aspects of the problem, invoking different physics and observations to investigate the issues for which they are most suited. Both techniques promise to contribute to our understanding of comets, though in different ways.

The strength of hydrodynamic models lies in their focus on more realistic physics in the gas flow under a given set of circumstances and assumptions. They are well-suited for theoretical studies that examine how different properties govern the formation of the near nucleus coma and for determining which properties have the most relevance and which may be neglected. They can also be developed to delve into particular scenarios, to investigate and test potential mechanisms that have been invoked for producing observed structures. In general, these models are most suitable for exploring the potential conditions that can exist in a coma, and for discovering how those different situations can be used to interpret the various types of morphology observed in comets.

However, hydrodynamic models are less suitable for solving for specific parameters in individual comets, an they are not generally extensible for use with ground-based observations. As described in Sec. 3.2, there are a large number of factors that can influence the gas flow in the inner coma, each of which introduces one or more free parameters into the analysis. Without in situ measurements to ascertain their values, most of these variables must be constrained remotely or assumed, which reduces the accuracy of the model, even though detailed physics are being used to trace the gas flows. As an example, the surface topography at all scales is critical for understanding the flow of the gas in the inner coma, yet for most comets, the nucleus shape is completely unknown, disqualifying them from detailed analyses. Even for those few comets visited by spacecraft (or whose shapes are inverted from lightcurves), the shapes are limited by the resolution of the model and the fraction of the nucleus that was constrained by flyby images, so the effects of topography are only partially accounted for. Furthermore, even when the shapes are known well enough to produce a partial solution, the lack of knowledge of the rest of the extensive parameter space means that, even if a solution is found to reproduce the observations, there is no guarantee that it is unique or truly representative of the conditions in the comet.

Collimated jet models were developed specifically for inferring various properties of the comet by reproducing the features observed in the coma. They adopt a simplified representation of the gas and dust emission to produce conceptual models, under the assumption that the jets remain collimated after they leave the nucleus. Though the jets are likely to be subject to the effects of gas dynamics within the first few nuclear radii, there is enough evidence that collimation is a controlling factor, especially in dust emission, to be confident that the models can produce meaningful results. There is another complication that must always be kept in

mind, however. The derived coma properties are strongly dependent on the interpretation of the features, whose appearance can be affected by the resolution of the images, projection effects, superposition of multiple sources, hydrodynamic interactions, image enhancements, etc. Thus, the accuracy of the results derived from these models must be recognized as being dependent on how well the morphology is understood. To reduce the ambiguities in the interpretation, different types of observations (spectroscopy, colors, polarization, etc.), or temporal coverage (e.g., movies) can prove extremely valuable for providing additional insight and for disentangling complex structures.

Even with the various qualifications, however, the collimated jet models have been tested and proven to work well at deriving nucleus properties. These tests have come from the models of the four comets that have been visited by spacecraft. In three of the four cases, the collimation models proved to be accurate at determining rotational properties, approximate source locations and properties of the jets. (The fourth, test was comet 1P/Halley, whose complex rotation state was difficult to pin down, even with multiple spacecraft observations.) The results from these models, discussed in detail in Section 6, prove that the collimated jet models, even with their minimalist representation of the coma physics, are a valuable tool for obtaining the some of the fundamental properties of a comet's nucleus.

4 Morphology as a Diagnostic Tool

The physical and dynamic properties of the nucleus govern the coma morphology; thus, measuring, understanding and modeling the observed phenomena provide a means of deriving nucleus properties. Currently, the collimated jet model is most commonly applied using Monte Carlo computer routines, which trace the outflowing dust/gas from discrete active regions on the rotating nucleus. Generally, models based on ground-based observations necessarily assume the nucleus is spherical to simplify interpretations (though in actuality, what is usually being modeled is the outflow from a spherical shell outside the nucleus where the dust and gas have decoupled and are in radial outflow). Matching the modeled structures to the observed coma for a given time and viewing geometry allows the determination of the nucleus and coma properties. It is generally possible (and prudent) to constrain a limited number of parameters (e.g., the spin axis direction and a primary source location) in early iterations, to minimize the parameter space being investigated. Subsequent simulations can then incorporate additional parameters to fine-tune and improve the solution. Some of the properties that can be determined from this modeling process include the rotation period and spin axis orientation (and possibly precession of the pole), the latitudes, relative longitudes and relative strengths of the active areas, opening angles of vents or surface extent of large active regions, ejection velocities of jet material, responses of the active regions to solar illumination, etc.

For the most part, model constraints have primarily come from visible observations of the dust coma, with the basic structures being interpreted and modeled as described in previous sections. However, technological developments, on a number of different fronts, have

significantly expanded the study and analyses of morphology, helping to constrain additional parameters and improving the understanding of what is seen. The availability of more and larger telescopes has increased the observational coverage of comets, so that short-lived and faint features can be captured and periodic changes can be monitored; the introduction of high-quality optics, including adaptive optics and space-based telescopes, improves the spatial resolution so that structures close to the nucleus can be resolved; the use of CCDs and spectral mappers allow data processing and image enhancement techniques to be employed; instruments spanning the spectral range from X-rays to radio wavelengths have been developed, offering different ways of investigating and interpreting features; polarization measurements are used to explore spatial variations in the dust properties throughout the coma; and the use of interplanetary spacecraft has made it possible to obtain in-situ observations and measurements, and relate the features to resolved images of the nucleus. We next discuss some of the techniques and describe how they are used in morphological studies to minimize ambiguities in the interpretation and to improve our understanding of the coma.

Temporal Changes. For many comets, temporal changes in the features provide basic nucleus information. Short-term periodic variations suggest a rotational modulation, with the time interval between repetitions revealing the comet's rotation period (Sekanina, 1981; Fomenkova et al., 1995; Schleicher et al., 1998; Schulz, 2002; Farnham et al., 2007a). Unlike many other properties, this result is independent of any model or of the mechanism that produces the structures (e.g., collimated jets, gasdynamic interactions). Short-term variations that do not seem to repeat may be indicative of a complex rotation, which is in itself an interesting result, though it makes it significantly more difficult to derive the rotation state (Belton et al., 1991; Jorda and Gutiérrez, 2000). Long-term changes are informative as well, though they are more representative of seasonal effects and provide constraints on the latitudinal distribution of active regions. Spontaneous features may also be observed, and can represent outbursts, fragmentation events, or short-term variability.

Fixed Jets. A fan or jet that appears unchanged for long periods of time is usually centered on the rotation axis (see Section 3.1). This configuration represents a special case that can be used to determine, with minimal modeling, the pole orientation of the nucleus in inertial space. The feature delineates the direction of the spin axis as projected on the sky, though in actuality, it may extend toward or away from the observer. Thus, the pole must lie somewhere on the great circle centered at the comet and passing through the observer and the feature. With two or more measurements from different viewing geometries (e.g., on different dates) multiple great circles are outlined, and the comet's spin axis is defined by the line at their intersection. Projecting this line out to the celestial sphere provides a measure of the pole orientation in inertial space. This is the most common procedure used to derive the spin axis information from morphology, because it requires little modeling and few assumptions.

Continuum Color. Simultaneous images of the continuum at different wavelengths can reveal spatial color variations across the coma, believed to be caused by difference in the dust particle sizes. Because dust grains tend to scatter light most efficiently at wavelengths comparable to their diameter (Bohren and Huffman, 1983; Jockers, 1997), larger grains will appear red-

der than small grains. A common observation is that jets and fans have a different color than the ambient coma, supporting the belief that there is a fundamental difference between the jet material and the rest of the coma. In most cases, jets are observed to be more blue or grey than their surroundings (Hartmann and Cruikshank, 1984; Kidger et al., 1998; Schulz and Stüwe, 2002; Schulz et al., 2005) indicating that the jets are composed of smaller grains (e.g., Kidger et al., 1998). This suggests that either the grains from active areas have an inherently different size distribution than from the ambient coma, or else the collimation mechanism (e.g., dust flowing through a vent or tube) batters the fragile grains, breaking them up before or shortly after they leave the nucleus. However, there are comets that have features that are redder than the surrounding coma (Hoban et al., 1989; Jockers and Bonev, 1997) and others where the features have the same color (e.g., Schulz and Stüwe, 2000). Radial color variations may also indicate an evolution of the dust as it expands away from the nucleus. Large grains near the nucleus give the inner coma a reddish color, which may become bluer at greater distances as the grains sublimate or fragment into smaller particles (Rousselot et al., 1992). More study is needed on this topic, to allow quantitative results to be obtained from the observations.

Albedo. Albedo maps of the coma are similar to color maps, except that they reveal spatial changes in the scattering and absorption properties of the grains. Rather than comparing observations at two different wavelengths where light is reflected, they compare the spatial distribution of reflected light to a second simultaneous observation of the coma's thermal emission. The spatial variations between the two observations can result either from compositional differences or structural differences in the grains. For a given composition, fluffier grains exhibit reduced albedos, because they induce multiple scattering events that allow more light to be absorbed. Albedo maps in most comets show lower albedo near the nucleus than farther out in the coma, indicating the presence of large, fluffy grains that fragment at larger distances (Telesco et al., 1986; Hammel et al., 1987).

Polarization. As with continuum color, polarization measurements also provide insight into the comet's dust properties. Sunlight scattered off small, irregular or aligned (via gas drag or electromagnetic forces) particles becomes linearly polarized, and the degree and characteristics of the polarization can be used to estimate the grain size and structure (Bohren and Huffman, 1983; Dolginov and Mitrofanov, 1976; Kolokolova and Jockers, 1997; Waldemarsson et al., 2000; Bertini et al., 2007). Although linear polarization has been studied in many comets, circular polarization has only recently been reliably measured. The interpretation of these measurements is still uncertain, but circular polarization may indicate the presence of organic material in the dust grains. Polarization can also be combined with coma color analyses to provide additional constraints (Jockers, 1997). Spatial variations are not uncommon, with jets and fans often standing out in polarized light (Levasseur-Regourd, 1999). This again suggests that there are fundamental differences in the porosity or fluffyness of the dust in the jet outflow. Furthermore, some jets are polarized but others are not, even in the same comet (Tozzi et al., 1997; Kelley et al., 2003), hinting about nuclear inhomogeneities. Radial variations are also seen in the ambient coma, where polarization is generally low near the nucleus and increases with distance (Levasseur-Regourd et al., 1993; Jewitt, 2004a). This reflects the behavior seen in color and albedo maps, supporting the conclusion that grains

are fragmenting into smaller particles as they recede from the nucleus.

Coma Shape, Asymmetry and Radial Gradients. As discussed in Section 2.1, the general shape of the coma is reflective of the comet's activity. The surface brightness of the coma falls off as a function of projected distance (ρ) from the nucleus, and in the case of a time-invariable dust outflow, this radial gradient profile will have a slope -1 (Gehrz and Ney, 1992). Deviations from this inverse-distance relationship reflect changes in the dust, where a number of different processes can cause the profile to steepen or flatten out (e.g., Jewitt and Meech, 1987; Jewitt and Luu, 1989; Boice et al., 2000; Tozzi et al., 2004). Dust acceleration or a lateral dust flow can increase the slope, while optical depth effects and extended or secondary sources act to flatten it. Depending on its exact nature, dust fragmentation or sublimation can increase or decrease the slope, and of course, modulation of the dust production rate can produce unusual changes in the profile. The radial gradient can be examined as an azimuthally averaged value or as separate profiles in different directions. A study is currently underway by this author to quantify how the different processes affect the coma, and to establish a means of exploring the evolution of the dust environment by using the characteristics of the radial profile (Farnham, 2007).

Gas Features and CHON Particles. Since first detected in comet 1P/Halley, gas features have become fairly common tools for exploring the nucleus properties. Because of the gasdynamics that tend to isotropize the gas flow, true gas jets may appear as simple asymmetries in the coma. As discussed in Section 3.1.2, however, well-defined gas jets are also often detected. These could be produced by some as-yet unknown collimation process, or they could be secondary emission from very small grains (often attributed to the CHON particles detected in the in situ measurements of comet 1P/Halley). If CHON grains are the correct interpretation, this presents an interesting issue for future investigations. The gas features are rarely coincident with the visible dust structures and sometimes even exist when little or no dust is detected, which means that the CHON particles are a population of organic grains or molecules that are not directly associated with the visible dust. They are assumed to be tiny because they accelerate to velocities approaching those of the gas and because they are undetected at visible wavelengths (other than by the secondary gas emission), yet they decouple from the gas early enough to remain in highly collimated jets.

An understanding of the physics behind the gas features is important, but even without it, the gas can be used to provide constraints in morphological studies. Regardless of how they are produced, the gas can be used in the same manner as dust jets, while bringing their own advantages to the analysis. The higher velocities in the gas flow cause the structures to appear at larger distances from the nucleus, so gas features often exhibit more detail than the dust features, especially in low resolution circumstances. This improves their measureability and makes them easier to interpret and model. Another benefit is that, not only are the gas features different from the dust features, but the features in one gas species are often different from those in another, revealing signatures of compositional inhomogeneites (Cosmovici et al., 1988; Boehnhardt and Birkle, 1994; Eberhardy et al., 2000; Lederer and Campins, 2002; Schulz, 2002; Lara et al., 2004; Feaga et al., 2007; Lin et al., 2007). If both dust and gas structures are observed in a comet, the results from the two components can

be combined to compare the derived properties for consistency and to determine if the gas issues from the same sources as the dust.

Even a gas coma that shows no features can be informative. Under the proper conditions, the coma's shape can be used to derive the scalelengths of the gas species, providing constraints for chemistry models (e.g., Fitzsimmons et al., 1990; Randall et al., 1992). This requires that the parent species are emitted directly from the nucleus, and that there is no extended emission, but if this is the case, then it is possible to obtain the parent velocities of the gases, as well as the dissociation velocities of the daughter species.

Night-Side Emission. Several recent comets have exhibited active regions that remain productive throughout a full rotation, even when the sources are unilluminated by sunlight. All four comets whose nuclei were imaged by spacecraft show evidence for emission arising from regions in darkness. These observations provide evidence for thermal lags in the nucleus, with energy being stored long enough to drive activity for many hours. Reconciling this evidence for a thermal lag with the low thermal inertia seen in comet 9P/Tempel 1 will help in understanding the thermal properties of the nucleus.

Indirect Detection of Structures. As discussed earlier, the lack of obvious features in the coma may be due to observational limitations, rather than to the absence of structure. There are a number of techniques that can be invoked as evidence of features, or for indirect detection of unresolved structures. Models of spectral line shapes may reveal periodic radial velocity shifts produced by nonisotropic emission on a rotating nucleus (Palmer et al., 1989; Schloerb and Lovell, 1998; Lecacheux et al., 2003). Color and polarization variations between the inner and outer coma may be a signature of unresolved jets (Goldberg and Brosch, 1995; Renard et al., 1996; Kidger et al., 1998). Nongravitational forces and changes in the rotation state have been used to derive the locations and strengths of isolated active regions (Yeomans et al., 2005; Gutiérrez and Davidsson, 2007). In situ dust measurements at comet 1P/Halley and 26P/Grigg-Skjellerup showed density concentrations and spatial variations of the dust properties that suggest they come from active areas on the nucleus (Vaisberg et al., 1987; Rabinowitz, 1988; Boehnhardt, 1989; Sekanina, 1991a; McBride et al., 1997). (In contrast, the dust "burst" measurements from comet 81P/Wild 2 and another event at 26P/Grigg-Skjellerup are thought to be fragmentation of large grains far from the nucleus.) Finally, a number of comets have been observed occulting stars, with increased extinction indicating higher density regions in the coma that are interpreted as dust jets (Combes et al., 1983; Hu et al., 1986; Ninkov, 1994; Elliot et al., 1995).

5 Comparison of JFCs to Other Comets

Jupiter family comets (JFCs) provide excellent opportunities for using coma morphology. They represent the best cases for detailed study because they can be observed over multiple apparitions, allowing comparisons from one orbit to another, and they are more likely to be targeted by spacecraft, which provides in situ measurements as "ground truth" for remote

sensing observations. JFCs also represent objects covering a broad range of evolutionary ages. Some have made hundreds of approaches to the Sun and should be highly altered, while others have never been perturbed into the inner solar system and should remain more pristine. Thus, the JFC class offers a variety of objects at different stages of maturity, and comprehensive studies of their properties could potentially provide clues to the changes that comets undergo as they age.

It is generally believed that, on average, JFCs are more highly evolved than other classes of comets. They should have experienced similar exposures to cosmic rays, UV photoprocessing, spallation and other prolonged sources of alteration as other families (Johnson et al., 1987; Strazzulla and Johnson, 1991), however, JFCs also receive more consistent solar irradiation than other classes of comet. The expectation is that over time, heating from repeated perihelion passages will deplete the volatiles near the surface of the nucleus, increasing the thickness of the mantle and reducing the comet's activity level. This does indeed appear to be the case, as older JFCs tend to exhibit lower production rates than those whose orbits have only more recently brought them close to the sun or dynamically new comets (Whipple, 1978; Luu and Jewitt, 1992; A'Hearn et al., 1995; Licandro et al., 2000; Tancredi et al., 2000). The assumption that JFCs are more highly evolved that other comets is clearly an oversimplification, however, because devolatilization depends strongly on the perihelion distance. Individual comets can vary significantly, depending on their particular histories. For example, an Oort cloud comet that passed within 0.5 AU of the Sun could have experienced more depletion of its surface volatiles than a JFC that has never gotten closer than 3 AU.

The specific ramifications of solar irradiation on coma morphology are not always obvious. On one hand, the increased mantle formation may choke off active areas and thus eliminate the coma features. On the other hand, mantle formation could predominantly act to shut off the isotropic component of the nucleus activity, while the concentrated emission from active areas keeps the vents clear (in effect enhancing the contrast of the jet structures). There is evidence that both effects occur, but because newer comets tend to have a stronger isotropic emission than older ones (Lien, 2002), it appears that the isotropic component of the coma disappears first, while jet activity can last much longer. As for distinct features, comparisons have yet to find any significant difference between the types of structure seen in JFCs and other classes of comets (e.g., Schulz, 2002; Ho et al., 2003; Kidger, 2004; Schulz et al., 2005; Schulz, 2008). This is only a preliminary result, based on a few focussed studies, and more comprehensive studies are needed to investigate the issue more fully.

It has been suggested that the lifetime of an active area is on the order of a few hundred orbits, based on erosion rates (Sekanina, 1990; Jewitt, 2004b), though this could vary depending the actual physical mechanisms that produce the activity and the evolution of the comet's orbit. Many JFCs have stable orbits that have brought them to small perihelion distances hundreds or thousands of times. Some of these comets exhibit no discernible features, which could indicate that any active regions that existed in the past have eroded away or mantled over. Others, such as comet 2P/Encke still consistently have structures, which means that either their sources are longer-lived than predicted (because they undercut the mantle instead of eroding downward?) or else they are forming new active areas. Other JFCs may also enter

periods of dormancy when certain volatiles are depleted from the surface, only to reactivate as the comet's orbit evolves closer to the Sun and new volatiles are able to begin sublimating.

6 Notable JFC Results

We now present discussions of some notable JFCs and what has been learned from their coma morphology. Particular emphasis is placed on 19P/Borrelly, 81P/Wild 2 and 9P/Tempel 1, because, as spacecraft mission targets, they represent test cases that can be used to evaluate the techniques used on other comets. Each one provides unique insight into how well the observations and models can be used under different circumstances. The other comets represent cases in which the techniques described earlier are applied to remote sensing data. It should be noted that numerous other JFCs also exhibit structures in their coma, but in many of these cases, there are not enough observations to usefully constrain the comet's physical properties.

6.1 Comet 19P/Borrelly

Comet 19P/Borrelly is a JFC that exhibits peculiar and interesting morphology. As discussed in Section 3.1.2, the coma is strongly dominated by a sunward-pointing, narrowly collimated jet (Fig. 2) that not only persists for several months around perihelion, but has been seen on all favorable apparitions since it was first detected in 1911. When this primary jet fades a few months after perihelion, a second feature becomes visible in the opposite direction, though it is significantly weaker and shows a slight curvature.

The constant nature of the primary structure over both long and short time scales, means that the main jet is aligned very closely with the spin axis of the nucleus, and that the nucleus is in, or very close to, a state of simple rotation. Using the great circle technique with the main jet, the spin axis was found to point to α=214°, δ=−5° (obliquity ∼100°) (Farnham and Cochran, 2002; Samarasinha and Mueller, 2002; Schleicher et al., 2003). This position in inertial space places the jet's source continuously in sunlight throughout the perihelion timeframe, with a minimum Sun angle of 10° about 6 weeks before perihelion. Unfortunately, the near-alignment of the jet and the pole hides any rotational modulation that would reveal additional information, so the morphology provides no constraints on the rotation period or the direction of spin. (Fortunately, Lamy et al. (1998) and Mueller and Samarasinha (2002) were able to derive a rotation period of ∼26 hr from lightcurves of the bare nucleus.) Historical descriptions and measurements of the jet were also used to derive the spin axis position over the past century. Results from as early as 1911 vary by less than about 8° from the 2001 solution, suggesting that any precession or drift of Borrelly's spin axis, though possibly real, is very small (Farnham and Cochran, 2002; Schleicher et al., 2003).

The Deep Space 1 spacecraft obtained a number of high-resolution images of comet Borrelly

that show features around the nucleus (Boice et al., 2000; Thomas et al., 2001; Soderblom et al., 2002; Soderblom et al., 2004). The collimated primary jet is clearly visible throughout several weeks of approach observations. In the highest resolution images (e.g., Fig. 9) the jet is seen to emanate from the central basin at the waist of the elongated nucleus, a location coinciding with the smallest axis of the nucleus, where rotation is most stable. Thus, the spacecraft observations confirm the ground-based assertion that the main jet is aligned with the spin axis. The DS1 observations also show several other structures. The second most prominent feature is a small fan jet emanating from the rounded end of the nucleus near the sub-solar point. There are also other small, collimated jets in the main jet, though they are skewed by about 15° from the main jet axis. None of these features is likely to be the secondary jet seen in the ground-based images, as the observations suggest that that source is on the opposite side of the nucleus and is unilluminated at the time of the DS1 flyby.

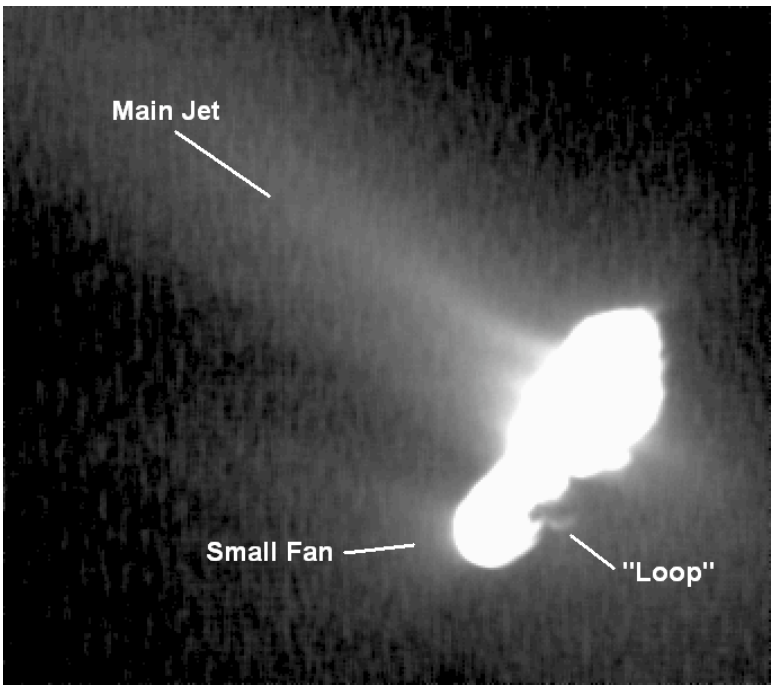

Fig. 9. Deep Space 1 image of the dust coma of comet 19P/Borrelly, showing the main collimated jet, the smaller secondary fan and the rapidly changing "loop" feature.

Another unusual feature seen in the DS1 images was a small, rapidly changing "loop" that was detected just above the terminator. Each of the images from close approach show this feature and, although it persists throughout the entire sequence, Fig. 10 shows that its appearance changes between each frame. The location and behavior of the loop indicate that it is produced by a source that is beyond the terminator on an unilluminated portion of the surface (Boice et al., 2000). The ejected material travels for a few seconds before rising into sunlight, where it is seen highlighted against the dark background. The rapid changes in its structure indicate that the source is variable on timescales as short as a minute or so. Though this structure is not fully understood, it is possible that the rapid changes are part of the shut-off process of an isolated source after it has rotated into darkness.

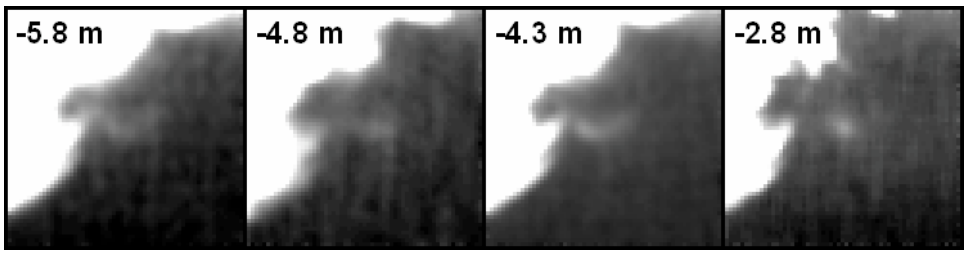

Fig. 10. Sequence of Deep Space 1 images zoomed in on the the rapidly changing "loop" structure in the coma of comet 19P/Borrelly. The saturated white region is the illuminated surface of the nucleus, while the "loop" at the center of each panel appears in the darkened region beyond the terminator. The time relative to closest approach is given in minutes.

An analysis of the radial profiles of the collimated jets shows that they remain nearly flat for the first 5 km or so, then fall off with a slope near -1, and become even steeper at even larger distances (Ho et al., 2003; Soderblom et al., 2004). This is interpreted as being caused by large icy grains being emitted in the collimated flow. These grains begin to sublimate and fragment a few seconds after leaving the nucleus and continue to fragment out to larger distances, producing a continuous cascade to ever smaller particle sizes.

The determination of the rotation state of the nucleus also offers the ability to derive secondary measurements. Schleicher et al. (2003) showed that the solar zenith angle relative to the primary source explains the comet's seasonal effect, where production rates peak before perihelion. The orientation and stability of the jet feature produced also explains Borrelly's nongravitational forces, which are larger than average, but have remained essentially constant since the comet was discovered. The emission of material in the collimated jet produces a strong recoil force that can perturb the comet's orbit, but because this force acts along the axis, it doesn't torque the nucleus, allowing a stable spin state. In an offshoot of the morphology results, quantitative analyses of the nongravitational forces were used to determine the mass and density of the nucleus (Farnham and Cochran, 2002; Davidsson and Gutiérrez, 2004).

6.2 Comet 81P/Wild 2

Comet 81P/Wild 2 has only recently been perturbed from a $\sim$40 year orbit into its current 6.4 year orbit, so it may be relatively new to the inner solar system, representing a more pristine stage of cometary evolution than many other JFCs. It was also not extensively observed until its 1996/1997 apparition, after it was selected as the target for the Stardust mission.

During the first half of this apparition, the coma exhibited a fan structure extending perpendicular to the sun-comet line, as shown in Fig. 1. This orientation indicates that it must be the result of nonisotropic emission rather than radiation pressure (which acts parallel to the comet's orbital plane). The fan remained visible from September 1996 through April 1997 with only gradual changes, and its constant appearance suggested that it was being

produced by a high-latitude source (Schulz et al., 2003; Farnham and Schleicher, 2005). It is not clear whether the fan is a wide source extending across the pole, or whether it is a cone swept out by a narrow jet offset from the spin axis, but there is no evidence of rotational modulation. After perihelion, the main fan disappeared, leaving a fainter, second structure in the opposite direction. This secondary source appears to be variable, as it is not seen on March 31 or April 25, but appears on April 2 and again on July 9. There is not enough temporal coverage to determine if this is rotational variability or intermittent activity. A dust tail was visible throughout the apparition, along with a faint anti-tail that suggests there are large grains in the coma.

As with comet 19P/Borrelly, the long-lived fan in comet 81P/Wild 2 was used to determine the orientation of the spin axis (arbitrarily designated as the North pole). Results from several groups (α=298°, δ=−5°, Sekanina, 2003; α=297°, δ=−10°, Vasundhara and Chakraborty, 2004; α=281°, δ=+13°, Farnham and Schleicher, 2005; obliquity ∼70°) agree surprisingly well, given the range of observations used to constrain the models. The narrow opening angle of the fan suggests that its source is located within ∼15° of the pole. The secondary source is likely to be at a mid-latitude on the opposite hemisphere, though it is not well constrained. The pole orientation is such that the primary source is continuously illuminated for several months before perihelion. This explains the seasonal effects, with the production rates peaking 80 days before perihelion. Because there is no rotational modulation detected in the ground-based images, neither the rotation period nor the sense of rotation could be determined. Color maps of the coma show no variations between the features and the ambient coma (Schulz et al., 2003; Farnham and Schleicher, 2005). Thus, the dust in the jets seems to have the same general characteristics as those in the rest of the coma, at least at the large distance scales measured. The radial profiles show that the primary jet has a slope significantly steeper than −1, indicating grains that are changing with time, while the secondary jet seen later in the apparition exhibits a slope much closer to the canonical value.

During the 2003/2004 apparition, the geometric conditions were extremely poor for Earth observations, so few ground-based measurements are available for this apparition. However, on January 2, 2004, the Stardust spacecraft flew through the coma of comet 81P/Wild 2, collecting dust grains to be returned to Earth. During this encounter, dozens of images of the nucleus and coma were obtained by the spacecraft, and these can be used to evaluate the results obtained from ground-based studies on the previous apparition.

The nucleus is closely approximated by a triaxial ellipsoid. If its shortest axis is assumed to correspond to the spin axis, as would be expected for an unexcited spin state, then the pole lies in the direction α=290°, δ=+13° (Brownlee et al., 2004b; Duxbury et al., 2004). A more rigorous triangular plate model of the visible portions of the nucleus produces similar results, with the axis pointed in the direction α=292°, δ=+17° (Kirk et al., 2005). These results are consistent with the solutions obtained from the ground-based measurements to within the uncertainties (typically ∼10°).

During the encounter, dozens of small, collimated dust jets were observed to emanate from various regions on the nucleus (see Fig. 11; Brownlee et al., 2004a). Because the encounter

took place about 3 months after perihelion, the sub-solar latitude was around −30°— too far south to illuminate the source for the main fan jet. Although this was fortunate for the safety of the spacecraft, it means there is no way to test the derived location of the fan's source. However, for 20 of the observed jets, Sekanina et al. (2004) used the parallax in different images to project the features back and determine where they intersect the triaxial ellipsoid model of the nucleus, with some interesting results. Two of the jets originate from regions on the nucleus that are unilluminated, again suggesting that there is a time lag that allows dust production to continue, even when the Sun is no longer driving the activity. Other features converge to higher albedo spots on the surface or to topographic shapes on the surface, though there is no consistent property in common for all the jets.

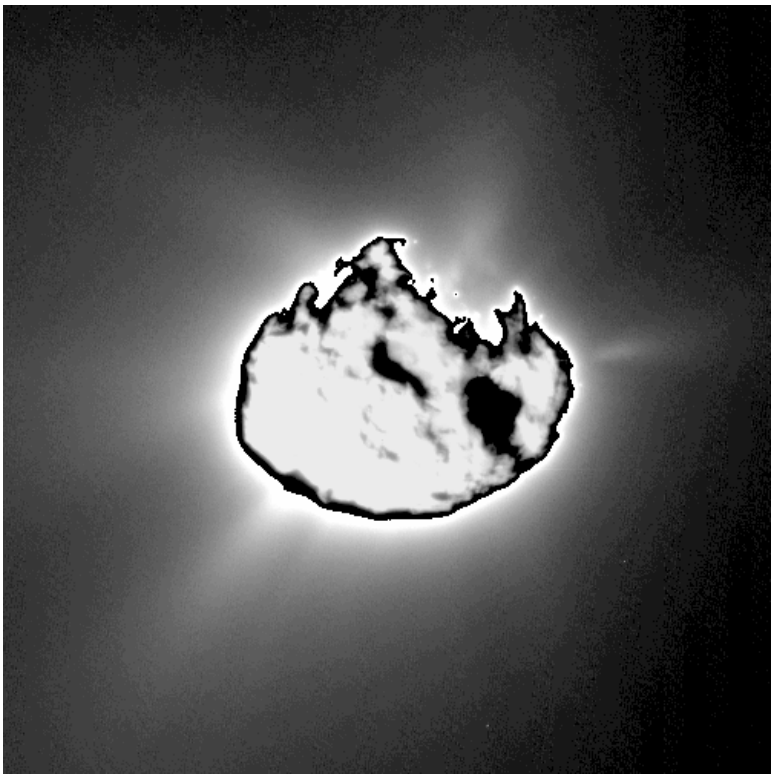

Fig. 11. Stardust image showing the nucleus and coma of comet 81P/Wild 2. Numerous radial jets are visible, including at least two that originate from regions of the nucleus that are in darkness (extending to the upper right). The nucleus is overlaid with a different scaling to reveal its details.

Sekanina also extrapolates the features outward and finds about a dozen potential occasions where the Stardust spacecraft may have passed through a stream of jet material. The approximate timings of several of these crossings correspond to regions where the dust flux monitor measures higher dust densities. (These crossings have spatial scales of hundreds of kilometers, as opposed to the one kilometer scale outbursts that are believed to be large grains fragmenting into their constituent particles in the coma.) Comparing dust fluxes in these high density regions to those in other portions of the spacecraft's path may represent a means of indirectly sampling the properties of different active regions across the surface.

If we use the 1996/1997 observations as representative of the comet's behavior, then we understand that the primary fan is in perpetual darkness at the time of the encounter, but the secondary jet may have been illuminated. However, all of the features seen in the encounter images are relatively small, which probably indicates that the secondary source was also inactive during the encounter. (We note that the few ground-based observations available from around the time of the Stardust encounter (e.g., Farnham and Schleicher, 2005) show no features other than the dust tail, though the observing conditions are very poor.) An alternative scenario is that the superposition of many small jets acts to mimic a single feature when seen at lower resolutions. If this were the case, then this would reinforce the caution that solutions derived from features are strongly dependent on the correct interpretation of those features.

6.3 Comet 9P/Tempel 1

Comet 9P/Tempel 1 is currently the best object available for comparing results from ground-based observations to those obtained in situ. In support of the Deep Impact mission, astronomers around the world monitored the comet for months before the event, using a variety of instruments and observing techniques. Furthermore, the spacecraft observed the comet for nearly two months before encounter, providing a long-term record of the temporal variations. Collectively, these observations provide a wealth of data for exploring the relationship between the coma and the nucleus.

The 5.5 year orbital period of Tempel 1 presents the Earth with alternate favorable and unfavorable apparitions. The 1999/2000 apparition, the first after the comet's selection as the DI target, was a poor one, so prior to the 2005 apparition, the only reported structures were an asymmetric coma and a fan-shaped feature (e.g., Walker et al., 1992; Fernández et al., 2003). Early in the 2005 apparition, continuum observations showed the asymmetric coma, which evolved into a fan several months before perihelion, distinguishable from the dust tail because it consistently pointed South of the orbital plane (e.g., Barnes et al., 2005; Farnham et al., 2005; Woodney et al., 2005; Lara et al., 2006). The fan was brightest and best defined about two months before perihelion, around the time the production rates peaked (Schleicher et al., 2006). Even though the rotation period was known to be 41 hr (A'Hearn et al., 2005), the fan remained stable, changing only on timescales of a month or so, which suggests that the source of the fan must be located near the spin axis. This result, along with the fact that the fan points to the south of the orbital plane leads to the conclusion that the nucleus must have a small obliquity (Lara et al., 2006; Schleicher et al., 2006; Keller et al., 2007, Samarasinha, private communication). The comet's nongravitational forces, strongest in the direction normal to the orbital plane (Yeomans et al., 2005), are consistent with this scenario. By April 2005, the southern fan had faded significantly from its peak, though it was still the brightest portion of the coma. Also during this time, enhanced images began to reveal radial features extending outward from the nucleus (Lara et al., 2006; Boehnhardt et al., 2007), and although they changed gradually, they continued to be detected until the time of the DI event. Under the assumption that they are the edges of emission cones, these

linear structures suggest that there are as many as 3 or 4 significant sources on the nucleus.

Observations of the gas coma (specifically CN) also reveal a southward jet, but it displays a different form than the dust fan, and shows variations on timescales of hours (Farnham et al., 2005; Schleicher et al., 2006; Boehnhardt et al., 2007). Although the observations were too sparse to independently derive a rotation state, these CN features exhibited changes consistent with the 41 hr rotation period and confirmed that their source was located near the pole.

The extensive monitoring of Tempel 1 shows that the radial gradient of the coma changed with time (Lara et al., 2006; Farnham et al., 2007b; Milani et al., 2007). Early in 2005, the coma falloff was consistently much steeper than the canonical value, so the dust was evolving dramatically after leaving the nucleus. However, as the comet neared perihelion, the coma gradient approached a slope of -1. Thus, grain behavior was changing, either due to differences in the effects of solar irradiation or to seasonal effects shifting the active areas on the nucleus.

Spatial polarization measurements show a low degree of polarization in the coma, with the fan being indistinguishable from the rest of the coma. Observations in conjunction with a broadband R filter do show some small variations that correspond to the linear structure in the inner coma (Hadamcik et al., 2007), however, this observation is in conflict with the lack of features seen in at longer wavelengths in Gunn i' filter images (Furusho et al., 2007). Though the observing conditions are similar in the two data sets, the discrepancy could be due to differences in signal-to-noise, or possibly to contamination of unpolarized gas emissions in the R filter.

The Deep Impact approach and encounter data is an excellent example of how resolution can play a major role in detecting and analyzing coma morphology. Unlike the DS1 and Stardust missions, the DI Medium Resolution Instrument (MRI) observations began two months before encounter and were obtained at 4 hour intervals (with increased sampling around the time of encounter), providing a continuous data set that links the distant, low resolution observations to the highest resolution images from encounter (Farnham et al., 2007b). In the first images from early May 2005, the southern fan was the only feature seen. As the range decreased, a small, narrow feature appeared to the northeast, then the southern fan was resolved into a series of arcs (which were in actuality segments of the conical spiral forming the fan). Temporal sequences show the arcs expanding outward as the nucleus rotates with the 41 hr period. The northeast feature was fainter, but proved to be the edge of a second cone, produced by a pair of jets at a common latitude on the opposite hemisphere.

The comet's pole orientation and direction of rotation were derived in conjunction with the shape model (α=294°, δ=+73°; Thomas et al., 2007). This pole position gives an obliquity of only $\sim$12° which agrees with the ground-based assertion that the pole is nearly perpendicular to the orbital plane. Given this solution, the northern sources are near +40° latitude, and the southern fan is produced, at least partly, by a jet near $-45°$ (Farnham et al., 2007b),

which also agrees with the ground-based observations. We note that the peak in gas and dust production ∼80 days before perihelion (Schleicher et al., 2006) suggests that the most productive active area on the surface has shut down by the time of the DI encounter, and the sub-solar latitude of +11° suggests that the inactive source is probably in darkness near the south pole. Unfortunately, the absence of a signature from this source in the DI observations means that the details regarding its location can't be well constrained. It might be that the jet at −45° originates from the northernmost edge of an extended active area or an entirely separate active region could lie closer to the pole.

Shortly before closest approach, the nucleus was resolved, along with numerous radial features (see Fig. 12; Farnham et al., 2007b). The surface brightness is dominated by the broad southern fan, but a narrower jet lies in the sunward direction and several fainter jets extend to the North. The three dimensional structure of these features can be derived using the parallax obtained from stereo pairs of observations (either two flyby images from different viewing directions, or an image from the flyby spacecraft and another from the impactor spacecraft). Work is currently underway to use the parallax information to project these features back to locate their points of origin on the nucleus.

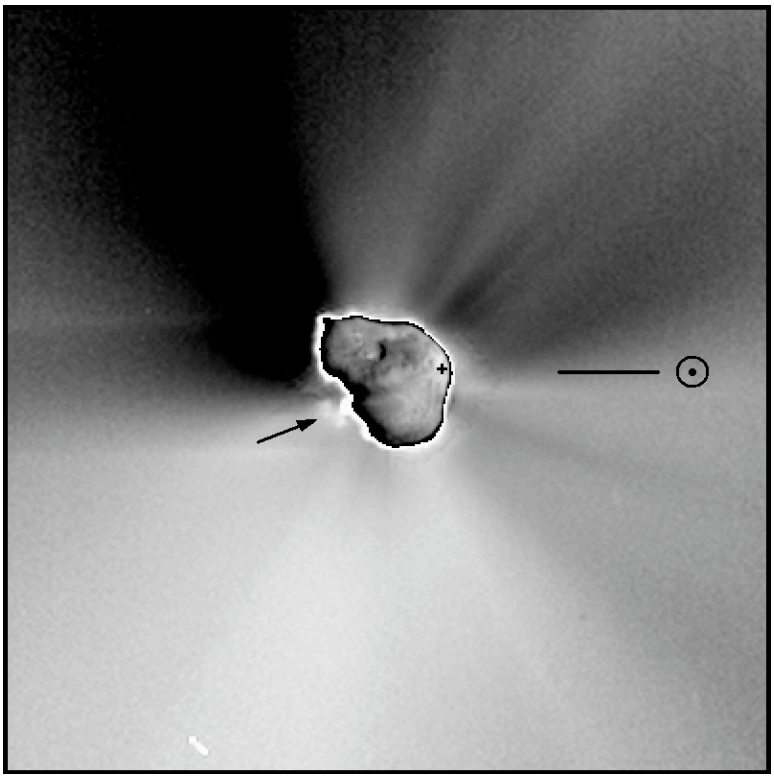

Fig. 12. Deep Impact image of the nucleus and dust coma of comet 9P/Tempel 1 (Farnham et al., 2007b). The bright southern fan extends toward the bottom of the image, and numerous intricate features radiate in all directions. The arrow denotes night-side features that emanate from just beyond the terminator. The nucleus is overlaid with a different scaling to reveal its details, and the "+" shows the approximate location of the sub-solar point.

There are a couple of structures of particular interest in the high-resolution images. Near the northern limb, small (∼10 m across), narrow jets are seen extending from the surface of the nucleus. Figure 8 shows that, as the flyby spacecraft passed under the nucleus, these jets appear to cross over the upper horizon, and these motions were used to approximate the source of the emission (Farnham et al., 2007b). It is clear that these small jets are in some way associated with the patches of surface water ice identified by Sunshine et al. (2006). The jets seem to project from near the edge of the ice patch in each case, rather than from the center or the full extent of the patch. This suggests that the jet and the ice patches are probably both produced by the same mechanism (rather than one causing the other). One potential scenario is that there are several sub-surface vents in the region, with the jets representing the dust entrained in the gas outflow, and the ice patches resulting from water recondensing on the surface around the vent during the night. Further analysis is needed to investigate the phenomenon in more detail.

The second feature of interest is located just beyond the terminator near the South pole (Fig. 12). Several bright clouds can be seen isolated against the dark background. These appear to be dust emanating from a source on the night side of the nucleus, with the plume rising above the local horizon into sunlight. As with comets 19P/Borrelly and 81P/Wild 2, activity from a source that is not in direct sunlight holds implications for the thermal properties of the nucleus material. After the DI impact, this region of the nucleus was indirectly illuminated by light reflected off the ejecta plume. Comparing the dust features to the surface topography, it appears that the night-side jets originate from around the edge of a scarp, suggesting that activity could be generated from nearly vertical surfaces that undercut the mantle, as described in Section 3.1.1. (Several kilometers of scarp, 20 m high and eroding back by about 50 m would produce the activity seen throughout an entire orbit of Tempel 1 (A'Hearn et al., 2005; Bensch et al., 2006).)

In addition to the dust coma, DI obtained images of the gas coma. Narrowband filters were used to image the coma during approach, and these images are currently being analyzed to determine the structure of the CN, C_2 and C_3 (McFadden et al., 2006). During the DI encounter, the slit on the Infrared Spectrometer was also scanned across the coma and nucleus, and these scans are used to create images at different wavelengths. Figure 7 shows the H_2O and CO_2 comae, with different features identifiable in each species (Feaga et al., 2007). Interestingly, the structure of the H_2O is different from that in the CO_2 and neither gas species exactly matches the dust features. The water emission is predominantly in the sunward direction, though it is not centered at the sub-solar point, while the CO_2 is strongly concentrated to the south.

Monitoring of comet Tempel 1 not only showed periodic variations in the coma, but also a number of transient outburst events, observed from Earth and HST as well as the DI spacecraft (Lara et al., 2006; Feldman et al., 2007). These spontaneous outbursts tend to occur at preferred rotational phases (Farnham et al., 2007b), suggesting that they are related to particular properties and illumination conditions on the nucleus, yet they do not occur on every rotation and the appearance (and even the direction) of the ejected material can vary dramatically, even for outbursts at the same rotational phase.

Finally, the impact of the DI probe produced another transient event that was observed worldwide, and analyses of the event reveal some interesting results. The dust ejected in the impact remained in the vicinity of the nucleus for several days, with the coma returning to pre-impact conditions after about six days. Models of the ground-based images indicate that the dust grains were typically micron-sized, with ejection velocities between 150 and 250 m s^{-1}, depending on when and where the measurements were taken (Schleicher et al., 2006; Feldman et al., 2007; Keller et al., 2007; Lara et al., 2007; Manfroid et al., 2007). Initial observations of the gas showed the same basic appearance as the dust ejecta, but expansion velocities 5-10 times higher. The CN and other species returned to pre-impact levels after only a day or so, while the dust took many days to dissipate, so any grain sublimation must have taken place in the first few hours after the impact.

In relation to coma morphology, another important result of the DI experiment was the lack of any continued emission after the initial event. All evidence points to the conclusion that, even though the impact punched a 200 m hole through the mantle, it had little lasting effect on the comet's normal activity. (e.g., Keller et al., 2007; Mäkinen et al., 2007; Schleicher, 2007; Weiler et al., 2007). It's possible that the impactor hit a relatively depleted area of the surface, that the opening quickly sealed itself off (e.g., ejecta falling back into the crater) or that the vent did remain active but its contribution was just too small to be detected against the comet's normal activity (even if only a few percent of the comet's $\sim$450 km^2 of surface area is active, it is still orders of magnitude larger than the $\sim$0.1 km^2 of crater area). In any case, the result has implications on how difficult it may be to introduce new active areas on a comet.

6.4 Comet 2P/Encke

Comet 2P/Encke is historically the most frequently observed JFC, having been observed on almost every apparition since it was determined to be a periodic comet in 1818. Its 3.3 year orbit is very stable, yet even after thousands of passes to within 0.33 AU of the sun, the comet is still active, showing that JFCs may have very long lifetimes before they become completely inactive. (Comets may go through periods of dormancy, only to become active again when their orbits have shifted further into the inner solar system, and 2P/Encke may be in one of these newly active phases (Kresak, 1987; Wetherill, 1991).) 2P/Encke's activity is somewhat unusual, however, with higher production rates around aphelion than at perihelion, and this seasonal effect, combined with repeatable coma features indicates that there is a protective mantle covering the surface. Historically, a sunward fan has been observed on every third or fourth apparition (e.g., Sekanina, 1988a,b), though with improvements in observing technology, it has been seen more frequently, appearing 2–3 months before perihelion, and disappearing shortly before perihelion. Given the reproducibility of this fan, it is probably present on every apparition, but may not be detectable due to observing circumstances (e.g., the Earth is inside the cone) or unfavorable geometry (the comet's 3.3 year orbit causes a roughly 10 year cycle of 3 orbits, in which the comet is visible pre-perihelion on one apparition, post-perihelion on the second, and essentially unobservable due to small solar

elongations on the third). Features tend to be absent in the post-perihelion timeframe, though there is one report of a distinct jet observed about six months after perihelion (Kelley et al., 2004).

The sunward fan is usually associated with the continuum observations (e.g., Butterworth, 1984; Kelley et al., 2004), and the lack of silicate features in its spectrum suggests it is composed of large grains (Kelley et al., 2004). (A dust trail of millimeter-sized grains extending around the comet's orbit provides additional evidence for large grains (Gehrz et al., 2004; Kelley et al., 2004).) The fan is usually seen even without image enhancements, so the material comprising it represents a significant portion of the comet's dust emission. Jewitt (2004a) use polarization maps to show that the fan is more highly polarized than the rest of the coma, with the degree of polarization increasing with distance from the nucleus. Similarly the dust colors are redder in the inner fan and become bluer with distance. These factors indicate that the dust is changing on timescales of hours, and the behavior is consistent with large fluffy grains disaggregating as they recede from the nucleus. Kiselev et al. (2004) also find a higher polarization in the fan, but they see a decrease in the degree at larger distances from the nucleus. The difference is likely due to gas contamination of the observations, which were obtained with broadband filters. (Though they attempted to correct for the NH emission, there are a number of other contaminants, and in a gas-rich comet the unpolarized gas emissions will dominate the outer coma.)

The fan is also detected in measurements of the gas. Photographic plates capturing wavelengths where emission from multiple gas species is strong show a much more rounded shape than plates restricted to the continuum (Djorgovski and Spinrad, 1985), International Ultraviolet Explorer (IUE) maps of OH in the coma reflect the asymmetric fan shape seen at visible wavelengths (Feldman et al., 1984; Festou and Barale, 2000), and long-slit spectra of the coma show dramatic asymmetries in the gas emission along the fan axis (Cochran, 2004). Thus, either the gas comes from the same source as the dust, or the fan is an extended emission source, with large grains emitting gas in the coma.

Sekanina (1988a,b) produced the first derivation of 2P/Encke's rotation state, using the great circle solution on measurements of the fan from 1868-1984. Results from these analyses found a pole orientation around α=205°, δ=+2°, (obliquity ∼70°) with the fan's source region at +55° latitude. Festou and Barale (2000) attempted to model the gas coma, as it was observed in 1980, using non-isotropic emission. They found that emission from the subsolar point could not reproduce the observations and instead preferred a source on a rotating nucleus (with the spin axis oriented near α=198°, δ=0° and the source at a latitude of 50°). More recently, Woodney et al. (2007) used the close approach of Encke in 2003 to obtain observations of the fan using narrowband filters to isolate the CN emission. The spatial scales were good enough to reveal a corkscrew morphology (Fig. 13), proving that the fan is indeed a cone of material centered on the spin axis. The great circle solution was applied to the corkscrew to derive a pole orientation of α=218°, δ=+9°, with a source at +70° latitude. The agreement between these different solutions suggests that, as with comet 19P/Borrelly the spin axis may be gradually drifting with time, but for the most part, 2P/Encke's nucleus is in a state of simple rotation.

Fig. 13. CN image of comet 2P/Encke, showing the corkscrew detail in the sunward fan, extending to the upper right. The coma has been enhanced by division of an azimuthally averaged profile and the "+" denotes the optocenter.

The derived solution explains the seasonal effects in the comet's activity as well as the pre-perihelion fan. Given the comet's orbit and the pole orientation, the sub-solar latitude remains above 40° for well over a year before perihelion, then rapidly moves South, crossing the equator about a week before perihelion. Thus, the high latitude source remains continuously illuminated during the entire inbound leg of the orbit, and moves into continuous darkness just before perihelion. The lack of activity after perihelion indicates that the southern hemisphere is heavily mantled due to repeated heating of the surface at small heliocentric distances. Only three months after perihelion, the Sun again crosses the equator moving North, and the high-latitude source again becomes illuminated. It is likely that this same active area is the source of the dust feature seen six months after perihelion (Kelley et al., 2004).

The rotation period of comet 2P/Encke has been difficult to define, as lightcurves from different epochs have produced different results, with measurements from the 1980s showing periodicities around 15 hr and more recent measurements showing 11 hr. Belton et al. (2005) present a discussion of the lightcurve analyses that we will not reproduce here, but a new and interesting twist has arisen and we note it here because it was derived from the coma morphology. From their 2003 observations, Woodney et al. (2007) produced a lightcurve with a period of 11.07 hr. More importantly, however, their CN observations of the corkscrew show repetitive features that can be used to obtain an independent measure of the rotation period,

and models of the corkscrew as a function of time suggest that the period is only consistent with the 11 hr determination. This leads to the surprising conclusion that the nucleus has a single-peaked lightcurve, and thus has either an extreme albedo variations or an unusual shape.

6.5 4P/Faye

Comet 4P/Faye is a fairly innocuous JFC that tends to exhibit a featureless, but asymmetric coma. The particle size distribution ranges from small silicate particles, evidenced by features in the spectrum (Hanner et al., 1996), to large grains that produce a long-lived dust trail (Sarugaku et al., 2007). However, the slope of the radial profile seems to remain near -1 in observations at different times and spatial scales (Jorda et al., 1995; Lamy et al., 1996), and color maps of the coma are neutral, (Grothues, 1996) suggesting that the dust is not changing significantly after it leaves the nucleus. Jorda et al. (1995) and Grothues (1996) used the apex distance in the sunward direction to compute dust velocities around 100-200 m s^{-1} for the smallest grains.

Given an active fraction $\sim$3%, Lamy et al. (1996) made an assumption that the asymmetry of the coma was due to a high-latitude source on the rotating nucleus, with the earth situated inside the cone that is swept out. By modeling the observed surface brightness, they found a pole orientation in the vicinity of α=215°, δ=+10° (obliquity $\sim$70°) with a source at +50° latitude. They do acknowledge that there are other interpretations for the asymmetry, and these may be more plausible, since a fan is never reported from outside the cone, even though observations are available for other times and viewing geometries.

6.6 Comet 7P/Pons-Winnecke and Comet 8P/Tuttle

Comets 7P/Pons-Winnecke and 8P/Tuttle both tend to be faint, with relatively low activity levels. They are both associated with meteor showers (the Boötid and Ursid meteor showers, respectively (Jenniskens, 2006)) indicating that, like many other JFCs, they emit large dust grains. Neither object is heavily studied and this, combined with the low activity, means that there are few reports of coma morphology. However, both comets have made close approaches to the Earth during which time features have been detected.

In 1927, 7P/Pons-Winnecke passed only 0.04 AU from the Earth, and for two months, a persistent sunward fan was visible. Sekanina (1989) used measurements of this fan to derive the pole orientation of the nucleus α=87°, δ=+54° (obliquity $\sim$60°).

In December 2007, comet 8P/Tuttle approached to within 0.25 AU of the Earth, and although it was not as close as Pons-Winnecke, observations of the gas coma showed multiple features (Schleicher and Woodney, 2007a,b). Intricate arcs were detected in images of the CN, C_2 and C_3, with at least three successive layers moving outward at 1.1 km s^{-1}. Schleicher and

Woodney used the spacing and the motions of these features to derive a 5.71 hr rotation period, the certainty of which is reinforced by the presence of multiple pairs of images, from various rotational cycles, that have matching structures.

6.7 Comet 10P/Tempel 2

A persistent sunward fan has been observed in comet 10P/Tempel 2 on many occasions (e.g., Jewitt and Luu, 1989; Boehnhardt et al., 1990). Sekanina (1991b) applied the great circle solution to measurements of the fan to compute a pole position α=147°, δ=+55° (obliquity 54°), with the source at a latitude higher than 60°. This result has accurately predicted the fan's position on every apparition since it was presented (e.g., Boehnhardt et al., 1990; Akisawa et al., 1992), which strongly indicates that the nucleus is in a state of simple rotation. The fan is also seen in images obtained in the thermal infrared (Campins et al., 1990) and in gas measurements (Boehnhardt et al., 1990; Spinrad, 1991). The spatial resolution in observations from the 1999 apparition were good enough to distinguish shell-like structures in the fan (Hergenrother and Larson, 1999), proving that it was formed by a jet on the rotating nucleus.

Comet 10P/Tempel 2 is one of the few comets for which a change in rotation rate has been confirmed. Sekanina (1991b) used lightcurve measurements to deduce a rotation period of 8.93 hr in 1988. On the next apparition in 1994, Mueller and Ferrin (1996) obtained measurements that were inconsistent with the 8.93 hr period (though there were several possible periods that fit the data). On the 1999 apparition, we obtained extensive observations that clearly show a period of 8.937 hr (20 s longer than the Sekanina result), which is inconsistent with any of the previous results, showing that changes are continuing. What makes this significant is that 10P/Tempel 2 has a larger-than-average nucleus that is active over only about 1% of its surface (Sekanina, 1988; A'Hearn et al., 1989; Jewitt and Luu, 1989). Additional study is needed to determine how the observed jet can produce sufficient torques to change the spin rate of a nucleus this large, but the implications for smaller nuclei are significant.

6.8 Comet 17P/Holmes

Comet 17P/Holmes was discovered in November 1892 during an outburst, and a second outburst followed in January 1893. In the apparitions over the intervening century, the comet was either not observed, or presented an unspectacular appearance. On October 23, 2007, 17P/Holmes experienced what may be the biggest ever recorded for a comet (Buzzi et al., 2007), increasing its brightness by 12 magnitudes in one day. In the outburst, a significant amount of dust was ejected (e.g., Montalto et al., 2008; Sekanina, 2008). Shortly after the event, a diffuse secondary condensation was detected near the nucleus, and both were surrounded by an expanding shell of dust and gas (Snodgrass et al., 2007). The nature of the secondary optocenter is currently undetermined. It could be a surface fragment, blown off in

the outburst, that continuously broke up, or it could simply be a cloud of low-velocity dust that slowly diffused away. Detailed modeling should be done to determine which scenario is most likely.

Over the next few months, the shell expanded rapidly (600 m s^{-1} at the leading edge) and the secondary condensation faded. Numerous streaks and rays were observed within the shell, some radiating from the nucleus, while others were more disorganized striae. Although many of these features appeared to be remnants of the ejected dust cloud, long-term monitoring revealed at least one jet that remained continuously active and varied periodically (Moreno et al., 2008; Trigo-Rodriguez et al., 2008). This outburst may then provide an example of a process (though arguably an extreme one) that could produce new active regions. Moreno et al. (2008) modeled the jet activity to derive an axis orientation α=39°, δ=+35° (obliquity 90°), with the jet's source near the south pole. With this orientation, the pole would have been pointed toward the sun at the time of the outburst, however, given the size of the outburst and the amount of material ejected, the rotational state could have been changed during the event. Furthermore, it is also possible that the nucleus is in a state of excited rotation, thus violating the assumption of simple rotation that was made in modeling the jet features.

After reports of the outburst, comet 17P/Holmes was extensively observed to investigate this unique event. Most of the data has yet to be fully analyzed, promising many interesting results are still forthcoming. The comet will also be of intense interest on its next few apparitions, to determine, among other things, if the jet observed after the outburst continues to remain active (to determine if a long-lived active region was uncovered) and if the nucleus exhibits excited rotation (possibly setting limits on the relaxation time). Observers will also be watching to see if any outburst activity is repeated.

6.9 Comet 22P/Kopff

There was little evidence for coma structures in comet 22P/Kopff between its discovery in 1906 and 1977, but strong nongravitational effects implied the presence of non-isotropic emission. Not only were the nongravitational forces strong, but the transverse component, which was positive around the time of the comet's discovery, reversed its sign around 1950 (Sekanina, 1984). This is generally agreed to be caused by a gradual drift or precession in the nucleus's rotation, and several studies have been done to model the variations and characterize the forces involved (Sekanina, 1984; Rickman et al., 1987; Yeomans and Chodas, 1989; Sitarski, 1994). Results from these studies differ depending on the assumptions that are made regarding the distribution of the activity that produces the jet forces.

After showing no morphology for so many of its early apparitions, in 1983 22P/Kopff began to exhibit structure in its coma. Beginning in 1983, Sekanina (1984) noted an asymmetric coma, while Cochran (1986) found the comet to have seasonal effects, showing higher activity before perihelion than after. After perihelion of the 1990 apparition, Farnham et al. (1996)

observed a broad fan pointed to the south of the orbital plane. The fan's 18 month persistence allowed the great circle technique to be used to compute a pole orientation in the vicinity of α=150°, δ=+85° (obliquity ∼25°). The comet has continued to exhibit a southern fan on subsequent passes, as reported by Cremonese and Rembor (1996) and Lamy et al. (2002) during the 1996 apparition and Miura et al. (2007) in 2003. The position of the fan in 2003 is inconsistent with that predicted by the Farnham et al. pole solution, which may indicate that the pole continues to precess.

6.10 Comet 67P/Churyumov-Gerasimenko

In 2014, the Rosetta spacecraft will rendezvous with the nucleus of comet 67P/Churyumov-Gerasimenko (67P/C-G), and will collect long-term, in situ observations while the comet approaches and recedes from the Sun. The extensive amount of data that will be obtained will make 67P/C-G the best test case for studies of come morphology (and virtually all other observational techniques). In preparation for the Rosetta rendezvous, ground-based observations are being obtained to characterize the behavior of the comet Unfortunately, 67P/C-G was selected as the Rosetta target well after the comet had passed perihelion in 2002, so observations from that apparition are limited. The 2009 perihelion passage, on the other hand, promises to provide extensive observations in support of the mission, and coma morphology will undoubtedly play a role in the analyses.

The active fraction of 67P/C-G is only about 6% (Kidger, 2003; Lamy et al., 2003) and the activity exhibits seasonal variations, with the OH and dust production peaking roughly a month after perihelion (Hanner et al., 1985; Kidger, 2004). Furthermore, the nongravitational forces are significant and appear to be consistent with the activity levels relative to perihelion (Chesley, 2004; Davidsson and Gutiérrez, 2005). These factors all suggest that the surface is highly mantled, with only a few small active areas. The observations from the spring of 2003 do indeed show several straight jet structures (Lamy et al., 2003; Schulz et al., 2004; Weiler et al., 2004; Lara et al., 2005), but by the time of the observations, they are small and not well defined. The morphology remains fairly constant throughout the observations, prompting the suggestion that the straight structures are the edges of a cone swept out by a narrow jet, but because the viewing geometry only changed by ∼15°, the great circle solution provides little constraint on the direction of the spin axis. Several pole solutions and limits have been dervived using different techniques, including two that involve the coma morphology (Chesley, 2004; Schleicher, 2006). Although neither of these solutions is tightly constrained, they are fairly consistent, falling within 18° of each other. They also both fall within the ranges of constraints from other techniques (Weiler et al., 2004; Davidsson and Gutiérrez, 2005; Lamy et al., 2006). Measurements of the coma's radial gradient show that it has a slope near the canonical value of −1, though it is not always constant with distance (Schulz et al., 2004; Lara et al., 2005; Lamy et al., 2006).

6.11 Comet 73P/Schwassmann-Wachmann 3

The series of nuclear fragmentation events experienced by comet 73P/Schwassmann-Wachmann 3 (73P/S-W3) offer the opportunity to explore many different aspects of cometary physics. The first signs of a nucleus breakup were seen in September 1995 (Crovisier et al., 1995; Bohnhardt et al., 1995), with four fragments ultimately detected. Fragments were again seen in 2000, though there was no evidence for continued breakup. The 2006/2007 apparition was particularly favorable, however, because the comet approached to within 0.08 AU of the Earth when it was near perihelion. During this encounter, the comet was observed to experience multiple cascading fragmentation events (Sekanina, 2007), which were observed by numerous observers worldwide. These observations will provide useful information about the exposure of fresh material, as well as providing constraints on the size distribution of the cometesimals that comprised the nucleus, and the dynamics involved in their breakup. Studies of 73P/S-W3 and other fragmented JFCs are addressed more fully by Fernández (2008).

Both dust and gas features were seen in the coma around a number of the fragments (e.g., Bonev et al., 2008) indicating that fresh ices are being exposed. The most widely observed fragments were C, which has apparently remained stable since the 1995 splitting, and B, which continued to breakup through the 2006 apparition. (In keeping with well-observed framentation events, two pairs of arclets were reported in fragment B (Lara et al., 2007)). Comparative studies of these two pieces will help our understanding of how fragments evolve after a breakup. Storm et al. (2006) are using high spatial resolution images of CN features to study the rotation state of fragment C, which seems to be in a state of simple rotation. Fragment B is undoubtedly in a state of complex rotation due to changes in its moment of inertia during the 2006 series of breakups, so future measurements of its spin state will provide constraints on the relaxation times for the excitation of the nucleus.

Polarization measurements and color maps of the different fragments also show that there are, not surprisingly, large dust grains that continue to fragment into smaller particles (Bonev et al., 2008; Ramos-Larios et al., 2008).

6.12 Comet 103P/Hartley 2

Comet 103P/Hartley 2 is different from most other JFCs, in that it appears to be active over a large fraction of its surface. Where most objects have an active fraction of less than 10%, measurements of 103P/Hartley 2 using various techniques have found active fractions ranging from 35% to greater than 100% (Groussin et al., 2004, and references therein). Because of the high active fraction, features are rarely detected in the coma of Hartley 2, though Suzuki et al. (1993) reported seeing CN and C_2 jets during the 1991 apparition, and models of the dust emission by Epifani et al. (2001) suggest that there is nonisotropic emission. More observations are clearly needed to fully characterize this comet's behavior.

It was recently announced that 103P/Hartley 2 is the new target for the Deep Impact Extended Investigation (DIXI), with an encounter currently scheduled for November 4, 2010. This is a fortunate development, in that it is an opportunity to obtain unprecedented observations of a comet with a large active fraction, which will provide important new information regarding mantle formation. The geometric conditions are favorable for Earth-based observations in the months before the encounter, with up to 10 hours of visibility per night, and a close approach to the Earth (0.12 AU) on October 21. Under these circumstances, the coma can be extensively monitored for months prior to the spacecraft flyby. Furthermore, the encounter will occur when the comet is only 0.15 AU from Earth, allowing high-resolution images of the coma to be obtained from Earth, maximizing the likelihood that features seen in the Earth-based observations can be linked to those in the spacecraft images.

7 Discussion

Jupiter family comets as a population present unique opportunities for detailed cometary studies. They represent a broad range of ages and evolutionary states, from young members that are relatively new to the inner solar system, to the oldest members that have seen thousands of perihelion passages. Because they have short orbital periods, they are more accessible than other classes of comet and can be observed on multiple apparitions (or even throughout an entire orbit). Not only does this allow for follow-up investigations to build upon previous discoveries, but new and better techniques can always be brought to bear to improve our understanding of the comet's behavior. The accessibility of JFCs also makes them logical choices for in situ spacecraft missions. Five of the six comets already visited by spacecraft, and all three targets of currently active missions are JFCs. These factors all contribute to the fact that members of the Jupiter family class are the most widely studied of comets.

Spacecraft observations provide the best constraints on cometary models and studies, but they are necessarily limited as to the number of objects that can be visited. Thus, one of the most valuable roles of these in situ measurements is to act as test data for calibrating and evaluating remote sensing techniques that can be applied to other comets. The techniques that use coma morphology to derive nucleus rotational properties have now been tested on three different JFCs (19P/Borrelly, 81P/Wild 2 and 9P/Tempel 1). In each case, the collimated jet models were highly successful in deriving rotational parameters consistent with the results determined from the spacecraft measurements. This imparts confidence that the techniques are valid for use in these studies and supports the presumption that they can reliably derive the properties of other comets. A list of JFCs, along with their derived rotational properties is given in Table 1. In each case, coma morphology played a role in determination of those rotation properties.

With rotational parameters being reliably measured, other techniques that utilize coma morphology should now be improved. Currently, radial gradient profiles, color maps, polarization

Table 1
JFC Rotation States Derived or Constrained by Coma Morphology

Comet	R.A.[1] (°)	Dec.[1] (°)	Obl.[2] (°)	Period[3] (hr)	Source
2P/Encke	205	+2	70		Sekanina, 1988a
	198	0	75		Festou and Barale, 2000
	218	+9	58	11.07±0.01	Woodney et al., 2007
4P/Faye	215	+10	70		Lamy et al., 1996
7P/Pons-Winnecke	87	+54	60		Sekanina, 1989
8P/Tuttle				5.7±0.04	Schleicher and Woodney, 2007b
9P/Tempel 1	294	+73	12	40.83±0.33	A'Hearn et al., 2005
10P/Tempel 2	147	+55	54		Sekanina, 1987b
17P/Holmes	39	+35	90		Moreno et al., 2008
19P/Borrelly	214	−5	102		Farnham and Cochran, 2002
	221	−7	99		Samarasinha and Mueller, 2002
	214	−6	103		Schleicher et al., 2003
22P/Kopff	120	+85	26		Farnham et al., 1996
67P/Churyumov-	90	+75	43		Chesley, 2004
Gerasimenko	223	−65	134		Schleicher, 2006
81P/Wild 2	298	−5	75		Sekanina, 2003
	297	−10	80		Vasundhara and Chakraborty, 2004
	281	+13	56		Farnham and Schleicher, 2005

[1] Right ascension and declination of the rotation pole.
[2] Obliquity of the rotation axis relative to the orbital momentum vector.
[3] Rotation period of the nucleus.

maps, albedo maps and other spatial variations are used to differentiate features and regions in the coma, with general descriptions put forth to explain the observations. As they currently exist, these techniques seem to work well as qualitative analysis tools, in that they tend to be self-consistent between themselves and in conjunction with spacecraft results (e.g., almost all lines of evidence suggest that grains fragment as they recede from the nucleus). However, future studies (including theoretical and laboratory investigations) should be developed to quantify the effects of the processes that bring about these coma variations, so that observed phenomena will lead to more concrete results regarding the properties of the dust and gas escaping from the comet. Studies involving polarization have been underway for some time, and the field has progressed to the point that measurements of the shape and degree of polarization can often be used to make specific conclusions about the dust characteristics.

Similarly, work is underway to model the evolutionary effects of the dust grains, to quantify their effects on the coma's radial gradient profiles. These studies are in their early stages, but could provide a basis for using observations of the coma shape to specify what processes are acting on the dust grains.

A final question that needs addressed is what produces the well-defined features detected in the gas images. If these are truly the result of highly collimated jets emerging from the nucleus, then what mechanism is producing the collimation? Alternately, if the features are produced by secondary emission from small dust grains, then what are the properties of these grains, and how might they relate to the CHON particles detected in the coma of comet 1P/Halley? Unfortunately, the resolution of this issue is not likely to be derived from ground-based observations, and, as with many other unanswered questions, must await the arrival of the Rosetta spacecraft at comet 67P/Churyumov-Gerasimenko.

References

A'Hearn, M. F., Belton, M. J. S., Delamere, W. A., Kissel, J., Klaasen, K. P., McFadden, L. A., Meech, K. J., Melosh, H. J., Schultz, P. H., Sunshine, J. M., Thomas, P. C., Veverka, J., Yeomans, D. K., Baca, M. W., Busko, I., Crockett, C. J., Collins, S. M., Desnoyer, M., Eberhardy, C. A., Ernst, C. M., Farnham, T. L., Feaga, L., Groussin, O., Hampton, D., Ipatov, S. I., Li, J.-Y., Lindler, D., Lisse, C. M., Mastrodemos, N., Owen, W. M., Richardson, J. E., Wellnitz, D. D., White, R. L., 2005. Deep Impact: Excavating Comet Tempel 1. Science 310, 258–264.

A'Hearn, M. F., Campins, H., Schleicher, D. G., Millis, R. L., 1989. The nucleus of Comet P/Tempel 2. Astrophys. J.347, 1155–1166.

A'Hearn, M. F., Festou, M. C., 1990. The neutral coma. In: Physics and Chemistry of Comets. pp. 69–110.

A'Hearn, M. F., Hoban, S., Birch, P. V., Bowers, C., Martin, R., Klinglesmith, D. A., 1986a. Cyanogen jets in Comet Halley. /nat 324, 649–651.

A'Hearn, M. F., Hoban, S., Birch, P. V., Bowers, C., Martin, R., Klinglesmith, III, D. A., 1986b. Gaseous jets in Comet P/Halley. In: ESLAB Symposium on the Exploration of Halley's Comet. Volume 2: Dust and Nucleus. Vol. 250 of ESA Special Publication. pp. 483–486.

A'Hearn, M. F., Millis, R. L., Schleicher, D. G., Osip, D. J., Birch, P. V., 1995. The ensemble properties of comets: Results from narrowband photometry of 85 comets, 1976-1992. Icarus 118, 223–270.

Akisawa, H., Tsumura, M., Nakamura, A., Watanabe, J.-I., 1992. Light curve and fan-shaped coma of Comet P/Tempel 2 in 1988-1989. In: Harris, A. W., Bowell, E. (Eds.), Asteroids, Comets, Meteors 1991. pp. 1–4.

Barnes, K., Baugh, N., Schleicher, D., Woodney, L., 2005. Gas and dust morphological results from narrowband imaging of Deep Impact's target Comet 9P/Tempel 1. Bull. Am. Ast. Soc.37, 1156.

Belton, M. J. S., Mueller, B. E. A., Julian, W. H., Anderson, A. J., 1991. The spin state and homogeneity of Comet Halley's nucleus. Icarus 93, 183–193.

Belton, M. J. S., Samarasinha, N. H., Fernndez, Y. R., Meech, K. J., 2005. The excited spin state of Comet 2P/Encke. Icarus 175, 181–193.

Bensch, F., Melnick, G. J., Neufeld, D. A., Harwit, M., Snell, R. L., Patten, B. M., Tolls, V., 2006. Submillimeter Wave Astronomy Satellite observations of Comet 9P/Tempel 1 and Deep Impact. Icarus 184, 602–610.

Bertini, I., Thomas, N., Barbieri, C., 2007. Modeling of the light scattering properties of cometary dust using fractal aggregates. Astron. Astrophys.461, 351–364.

Boehnhardt, H., 1989. Clusters and packets of grains in Comet Halley and the fragmentation of dust. Earth, Moon, Planets46, 221–226.

Boehnhardt, H., 2002. Comet splitting — Observations and model scenarios. Earth, Moon, Planets89, 91–115.

Boehnhardt, H., 2004. Split Comets. In: Festou, M. H., Keller, U., Weaver, H. (Eds.), Comets II. University of Arizona Press, Tucson, pp. 301–316.

Boehnhardt, H., Beisser, K., Vanysek, V., Mueller, B. E. A., Weiss, M., Jager, M., Reinsch, K., Grun, E., 1990. Direct imaging and spectrophotometry of Comet P/Tempel 2. Icarus 86, 58–68.

Boehnhardt, H., Birkle, K., 1994. Time variable coma structures in comet P/Swift-Tuttle. Astron. Astrophys. Supp.107, 101–120.

Boehnhardt, H., Pompei, E., Tozzi, G. P., Hainaut, O., Ageorges, N., Bagnulo, S., Barrera, L., Bonev, T., Käufl, H. U., Kerber, F., Locurto, G., Marco, O., Pantin, E., Rauer, H., Saviane, I., Selman, F., Sterken, C., Weiler, M., 2007. Broad- and narrowband visible imaging of comet 9P/Tempel 1 at ESO around the time of the Deep Impact event. Astron. Astrophys.470, 1175–1183.

Bohnhardt, H., Kaufl, H. U., Keen, R., Camilleri, P., Carvajal, J., Hale, A., 1995. Comet 73P/Schwassmann-Wachmann 3. IAU Circ. 6274.

Bohren, C. F., Huffman, D. R., 1983. Absorption and scattering of light by small particles. New York: Wiley, 1983.

Boice, D. C., Soderblom, L. A., Britt, D. T., Brown, R. H., Sandel, B. R., Yelle, R. V., Buratti, B. J., Hicks, M. D., Nelson, R. M., Rayman, M. D., Oberst, J., Thomas, N., 2000. The Deep Space 1 encounter with Comet 19P/Borrelly. Earth, Moon, Planets89, 301–324.

Bonev, T., Boehnhardt, H., Borisov, G., 2008. Broadband imaging and narrowband polarimetry of comet 73P/Schwassmann-Wachmann 3, components B and C, on 3, 4, 8, and 9 May 2006. Astron. Astrophys.480, 277–287.

Brandt, J. C., 1982. Observations and dynamics of plasma tails. In: Wilkening, L. L. (Ed.), Comets. Univ. of Arizona Press, Tucson, pp. 519–537.

Brin, G. D., Mendis, D. A., 1979. Dust release and mantle development in comets. Astrophys. J.229, 402–408.

Brownlee, D., Clark, B., Tsou, P., Kissel, J., Newburn, R., Tuzzolino, A., Anderson, J., Green, S., Hoerz, F., Sandford, S., 2004a. First results from the Stardust mission flyby of Comet Wild 2. In: 35th COSPAR Scientific Assembly. Vol. 35 of COSPAR, Plenary Meeting. p. 1165.

Brownlee, D. E., Horz, F., Newburn, R. L., Zolensky, M., Duxbury, T. C., Sandford, S., Sekanina, Z., Tsou, P., Hanner, M. S., Clark, B. C., Green, S. F., Kissel, J., 2004b. Surface

of young Jupiter family comet 81P/Wild 2: View from the Stardust spacecraft. Science 304, 1764–1769.
Butterworth, P. S., 1984. Physical properties of comets. Vistas in Astronomy 27, 361–419.
Buzzi, L., Muler, G., Kidger, M., Henriquez Santana, J. A., Naves, R., Campas, M., Kugel, F., Rinner, C., 2007. Comet 17P/Holmes. IAU Circ. 8886.
Campins, H., Decher, R., Telesco, C. M., Lien, D. J., 1990. Ground-based thermal IR images of Comet Tempel 2. Icarus 86, 220–227.
Campins, H., Rieke, G. H., Lebofsky, M. J., 1982. Infrared photometry of periodic Comets Encke, Chernykh, Kearns-Kwee, Stephan-Oterma, and Tuttle. Icarus 51, 461–465.
Chesley, S. R., 2004. An estimate of the spin axis of Comet 67P/Churyumov-Gerasimenko. Bull. Am. Ast. Soc.36, 1118.
Cochran, A. L., 1986. Comet Kopff - A case for mantle development. Astron. J.91, 646–649.
Cochran, A. L., 2004. Observations of Comet 2P/Encke during the 2003 apparition. Bull. Am. Ast. Soc.36, 1145.
Colwell, J. E., Jakosky, B. M., 1987. The evolution of topography on a comet. In: Lunar and Planetary Institute Conference Abstracts. Vol. 18 of Lunar and Planetary Institute Conference Abstracts. pp. 193–194.
Colwell, J. E., Jakosky, B. M., Sandor, B. J., Stern, S. A., 1990. Evolution of topography on comets. II - Icy craters and trenches. Icarus 85, 205–215.
Combes, M., Lecacheux, J., Encrenaz, T., Sicardy, B., Zeau, Y., Malaise, D., 1983. On stellar occultations by comets. Icarus 56, 229–232.
Combi, M. R., 1987. Sources of cometary radicals and their jets — Gases or grains. Icarus 71, 178–191.
Combi, M. R., 1996. Time-dependent gas kinetics in tenuous planetary atmospheres: The cometary coma. Icarus 123, 207–226.
Combi, M. R., Harris, W. M., Smyth, W. H., 2004. Gas dynamics and kinetics in the cometary coma: Theory and observations. In: Festou, M. H., Keller, U., Weaver, H. (Eds.), Comets II. University of Arizona Press, Tucson, pp. 523–552.
Combi, M. R., Kabin, K., Dezeeuw, D. L., Gombosi, T. I., Powell, K. G., 1997. Dust-gas interrelations in comets: Observations and theory. Earth, Moon, Planets79, 275–306.
Cosmovici, C. B., Schwarz, G., Ip, W.-H., Mack, P., 1988. Gas and dust jets in the inner coma of Comet Halley. Nature332, 705–709.
Cremonese, G., Rembor, K., 1996. Comet 22p/kopff. IAU Circ. 6521.
Crifo, J.-F., 2006. Multidimensional physicochemical models of the near-nucleus coma: Present achievements and requested future developments. Advances in Space Research 38, 1911–1922.
Crifo, J. F., Fulle, M., Kömle, N. I., Szego, K., 2004. Nucleus-coma structural relationships: Lessons from physical models. In: Festou, M. H., Keller, U., Weaver, H. (Eds.), Comets II. University of Arizona Press, Tucson, pp. 471–503.
Crifo, J. F., Itkin, A. L., Rodionov, A. V., 1995. The near-nucleus coma formed by interacting dusty gas jets effusing from a cometary nucleus. Icarus 116, 77–112.
Crifo, J. F., Rodionov, A. V., 1997. The dependence of the circumnuclear coma structure on the properties of the nucleus. Icarus 127, 319–353.
Crifo, J. F., Rodionov, A. V., Szegö, K., Fulle, M., 2002. Challenging a paradigm: Do we need active and inactive areas to account for near-nuclear jet activity? Earth, Moon, Planets90,

227–238.
Crovisier, J., Biver, N., Bockelee-Morvan, D., Colom, P., Gerard, E., Jorda, L., Rauer, H., 1995. Comet 73P/Schwassmann-Wachmann 3. IAU Circ. 6227.
Davidsson, B., 2007. Sub-surface cavities as sources of cometary jets. Bull. Am. Ast. Soc.39, 499.
Davidsson, B. J. R., Gutiérrez, P. J., 2004. Estimating the nucleus density of Comet 19P/Borrelly. Icarus 168, 392–408.
Davidsson, B. J. R., Gutiérrez, P. J., 2005. Nucleus properties of Comet 67P/Churyumov Gerasimenko estimated from non-gravitational force modeling. Icarus 176, 453–477.
de Sanctis, M. C., Capaccioni, F., Capria, M. T., Coradini, A., Federico, C., Orosei, R., Salomone, M., 1999. Models of P/Wirtanen nucleus: active regions versus non-active regions. Planet. Space Sci.47, 855–872.
de Sanctis, M. C., Capria, M. T., Coradini, A., 2003. Models of P/Borrelly: Activity and dust mantle formation. Advances in Space Research 31, 2519–2525.
Djorgovski, S., Spinrad, H., 1985. Surface photometry of comet P/Encke. Astron. J.90, 869–876.
Dolginov, A. Z., Mitrofanov, I. G., 1976. Orientation of cometary dust and polarization observations of comets. Soviet Astronomy 19, 758–764.
Duxbury, T. C., Newburn, R. L., Brownlee, D. E., 2004. Comet 81P/Wild 2 size, shape, and orientation. Journal of Geophysical Research (Planets) 109 (E18), 12.
Eberhardy, C. A., Woodney, L. M., Schleicher, D. G., 2000. Gas and dust jet morphology as a function of rotation in Comet Hyakutake (1996 B2) at perigee. Bull. Am. Ast. Soc.32, 1072.
Eddington, A. S., 1910. The envelopes of Morehouse (1908c). Mon. Not. R. Astron. Soc.70, 442–458.
Elliot, J. L., Olkin, C. B., Dunham, E. W., Ford, C. H., Gilmore, D. K., Kurtz, D., Lazzaro, D., Rank, D. M., Temi, P., Bandyopadhyay, R. M., Barroso, J., Barrucci, A., Bosh, A. S., Buie, M. W., Bus, S. J., Dahn, C. C., Foryta, D. W., Hubbard, W. B., Lopes, D. F., Marcialis, R. L., 1995. Jet-like features near the nucleus of Chiron. Nature373, 46–49.
Epifani, E., Colangeli, L., Fulle, M., Brucato, J. R., Bussoletti, E., de Sanctis, M. C., Mennella, V., Palomba, E., Palumbo, P., Rotundi, A., 2001. ISOCAM imaging of Comets 103P/Hartley 2 and 2P/Encke. Icarus 149, 339–350.
Farnham, T. L., 2007. Radial surface brightness profiles as diagnostic tools in cometary dust comae. Bull. Am. Ast. Soc.39, 524.
Farnham, T. L., Cochran, A. L., 2002. A McDonald Observatory study of comet 19P/Borrelly: Placing the Deep Space 1 observations into a broader context. Icarus 160, 398–418.
Farnham, T. L., Meech, K. J., Nassir, M., 1996. The dust tail of Comet P/Kopff. Bull. Am. Ast. Soc.28, 1084.
Farnham, T. L., Mueller, B. E. A., Knight, M. M., Samarasinha, N. H., 2005. Narrowband observations of Comet Tempel 1 in support of the Deep Impact mission. Bull. Am. Ast. Soc.37, 711.
Farnham, T. L., Samarasinha, N. H., Mueller, B. E. A., Knight, M. M., 2007a. Cyanogen jets and the rotation state of Comet Machholz (C/2004 Q2). Astron. J.133, 2001–2007.
Farnham, T. L., Schleicher, D. G., 2005. Physical and compositional studies of Comet

81P/Wild 2 at multiple apparitions. Icarus 173, 533–558.
Farnham, T. L., Schleicher, D. G., Woodney, L. M., Birch, P. V., Eberhardy, C. A., Levy, L., 2001. Imaging and photometry of Comet C/1999 S4 (LINEAR) before perihelion and after breakup. Science 292, 1348–1353.
Farnham, T. L., Wellnitz, D. D., Hampton, D. L., Li, J.-Y., Sunshine, J. M., Groussin, O., McFadden, L. A., Crockett, C. J., A'Hearn, M. F., Belton, M. J. S., Schultz, P., Lisse, C. M., 2007b. Dust coma morphology in the Deep Impact images of Comet 9P/Tempel 1. Icarus 187, 26–40.
Feaga, L. M., A'Hearn, M. F., Sunshine, J. M., Groussin, O., Farnham, T. L., 2007. Asymmetries in the distribution of H_2O and CO_2 in the inner coma of Comet 9P/Tempel 1 as observed by Deep Impact. Icarus 190, 345–356.
Feldman, P. D., McCandliss, S. R., Route, M., Weaver, H. A., A'Hearn, M. F., Belton, M. J. S., Meech, K. J., 2007. Hubble Space Telescope observations of Comet 9P/Tempel 1 during the Deep Impact encounter. Icarus 187, 113–122.
Feldman, P. D., Weaver, H. A., Festou, M. C., 1984. The ultraviolet spectrum of periodic Comet Encke (1980 XI). Icarus 60, 455–463.
Fernández, Y. R., 2008. Fragmenting JFCs. Planet. Space Sci. (this volume), 00–00.
Fernández, Y. R., Meech, K. J., Lisse, C. M., A'Hearn, M. F., Pittichová, J., Belton, M. J. S., 2003. The nucleus of Deep Impact target Comet 9P/Tempel 1. Icarus 164, 481–491.
Festou, M. C., Barale, O., 2000. The asymmetric coma of comets. I. Asymmetric outgassing from the nucleus of Comet 2P/Encke. Astron. J.119, 3119–3132.
Fitzsimmons, A., Williams, I. P., Williams, G. P., Andrews, P. J., 1990. Narrow-band photometry of Comet P/Halley - OH and H_2O scalelengths and pre-perihelion production rates. Mon. Not. R. Astron. Soc.244, 453–457.
Fomenkova, M. N., Jones, B., Pina, R., Puetter, R., Sarmecanic, J., Gehrz, R., Jones, T., 1995. Mid-infrared observations of the nucleus and dust of Comet P/Swift-Tuttle. Astron. J.110, 1866.
Fulle, M., Milani, A., Pansecchi, L., 1997. Tomography of a sunward structure in the dust tail of Comet 19P/Borrelly. Astron. Astrophys.321, 338–342.
Furusho, R., Ikeda, Y., Kinoshita, D., Ip, W.-H., Kawakita, H., Kasuga, T., Sato, Y., Lin, H.-C., Chang, M.-S., Lin, Z.-Y., Watanabe, J.-I., 2007. Imaging polarimetry of Comet 9P/Tempel before and after the Deep Impact. Icarus 190, 454–458.
Gehrz, R. D., Ney, E. P., 1992. 0.7- to 23-micron photometric observations of P/Halley 1986 III and six recent bright comets. Icarus 100, 162–186.
Gehrz, R. D., Reach, W. T., Woodward, C. E., Kelley, M. S., 2004. Spitzer infrared observations of comets. Bull. Am. Ast. Soc.36, 1434.
Goldberg, Y., Brosch, N., 1995. Imaging polarimetry of the comet P/Swift-Tuttle. Mon. Not. R. Astron. Soc.273, 431–442.
Gombosi, T. I., Cravens, T. E., Nagy, A. F., 1985. Time-dependent dusty gasdynamical flow near cometary nuclei. Astrophys. J.293, 328–341.
Gombosi, T. I., Horanyi, M., 1986. Time-dependent numerical modeling of dust halo formation at comets. Astrophys. J.311, 491–500.
Grothues, H.-G., 1996. Photometry and direct imaging of Comet P/Faye 1991 XXI. Planet. Space Sci.44, 625–635.
Groussin, O., A'Hearn, M. F., Li, J.-Y., Thomas, P. C., Sunshine, J. M., Lisse, C. M., Meech,

K. J., Farnham, T. L., Feaga, L. M., Delamere, W. A., 2007. Surface temperature of the nucleus of Comet 9P/Tempel 1. Icarus 187, 16–25.

Groussin, O., Lamy, P., Jorda, L., Toth, I., 2004. The nuclei of Comets 126P/IRAS and 103P/Hartley 2. Astron. Astrophys.419, 375–383.

Gruen, E., Bar-Nun, A., Benkhoff, J., Bischoff, A., Dueren, H., Hellmann, H., Hesselbarth, P., Hsiung, P., Keller, H. U., Klinger, J., 1991. Laboratory simulation of cometary processes — Results from first KOSI experiments. In: Newburn, Jr., R. L., Neugebauer, M., Rahe, J. (Eds.), IAU Colloq. 116: Comets in the post-Halley era. Vol. 167 of Astrophysics and Space Science Library. pp. 277–297.

Gutiérrez, P. J., Davidsson, B. J. R., 2007. Non-gravitational force modeling of Comet 81P/Wild 2. Icarus 191, 651–664.

Gutiérrez, P. J., Ortiz, J. L., Rodrigo, R., López-Moreno, J. J., 2000. A study of water production and temperatures of rotating irregularly shaped cometary nuclei. Astron. Astrophys.355, 809–817.

Gutiérrez, P. J., Ortiz, J. L., Rodrigo, R., López-Moreno, J. J., 2001. Effects of irregular shape and topography in thermophysical models of heterogeneous cometary nuclei. Astron. Astrophys.374, 326–336.

Hadamcik, E., Levasseur-Regourd, A.-C., 2003. Dust coma of Comet C/1999 S4 (LINEAR): Imaging polarimetry during nucleus disruption. Icarus 166, 188–194.

Hadamcik, E., Levasseur-Regourd, A. C., Leroi, V., Bardin, D., 2007. Imaging polarimetry of the dust coma of Comet Tempel 1 before and after Deep Impact at Haute-Provence Observatory. Icarus 190, 459–468.

Hammel, H. B., Telesco, C. M., Campins, H., Decher, R., Storrs, A. D., Cruikshank, D. P., 1987. Albedo maps of Comets P/Halley and P/Giacobini-Zinner. Astron. Astrophys.187, 665–668.

Hanner, M. S., Lynch, D. K., Russell, R. W., Hackwell, J. A., Kellogg, R., Blaney, D., 1996. Mid-infrared spectra of Comets P/Borrelly, P/Faye, and P/Schaumasse. Icarus 124, 344–351.

Hanner, M. S., Tedesco, E., Tokunaga, A. T., Veeder, G. J., Lester, D. F., Witteborn, F. C., Bregman, J. D., Gradie, J., Lebofsky, L., 1985. The dust coma of periodic Comet Churyumov-Gerasimenko (1982 VIII). Icarus 64, 11–19.

Harris, W. M., Combi, M. R., Honeycutt, R. K., Mueller, B. E. A., 1997. Evidence for interacting gas flows and an extended volatile source distribution in the coma of Comet C/1996 B2 (Hyakutake). Science 277, 676–681.

Hartmann, W. K., Cruikshank, D. P., 1984. Comet color changes with solar distance. Icarus 57, 55–62.

Hergenrother, C. W., Larson, S., 1999. Comet 10P/Tempel 2. IAU Circ. 7313.

Ho, T. M., Thomas, N., Boice, D. C., Boney, T., Jockers, K., Sonderblom, L. A., 2004. The dust coma of 19P/Borrelly. In: 35th COSPAR Scientific Assembly. Vol. 35 of COSPAR, Plenary Meeting. p. 1002.

Ho, T. M., Thomas, N., Boice, D. C., Kollein, C., Soderblom, L. A., 2003. Comparative study of the dust emission of 19P/Borrelly (Deep Space 1) and 1P/Halley. Advances in Space Research 31, 2583–2589.

Hoban, S., A'Hearn, M. F., Birch, P. V., Martin, R., 1989. Spatial structure in the color of the dust coma of Comet P/Halley. Icarus 79, 145–158.

Horanyi, M., Gombosi, T. I., Cravens, T. E., Korosmezey, A., Kecskemety, K., Nagy, A. F., Szego, K., 1984. The friable sponge model of a cometary nucleus. Astrophys. J.278, 449–455.

Hu, Z.-W., Chen, Y., Zhang, Z.-S., 1986. A preliminary analysis of a light curve of the occultation by comet P/Crommelin. J. Nanjing Univ. 22, 674–681.

Huebner, W. F., 2003. A quantitative model for comet nucleus topography. Advances in Space Research 31, 2555–2562.

Hughes, D. W., 1991. Possible mechanisms for cometary outbursts. In: Newburn, Jr., R. L., Neugebauer, M., Rahe, J. (Eds.), IAU Colloq. 116: Comets in the post-Halley era. Vol. 167 of Astrophysics and Space Science Library. pp. 825–851.

Ibadinov, K. I., 1989. Laboratory investigation of the sublimation of comet nucleus models. Advances in Space Research 9, 97–112.

Ibadinov, K. I., 1999. Growth of a refractory mantle on a cometary nucleus and the evolution of the nucleus into an asteroid-like body. Solar System Research 33, 319–323.

Ibadinov, K. I., Rahmonov, A. A., 2002. Laboratory studies of gas-dust jet formation on cometary nucleus surface. Advances in Space Research 29, 705–708.

Ivanova, A., Shulman, L., 2002. A model of an active region on the surface of a cometary nucleus. Earth Moon and Planets 90, 249–257.

Jehin, E., Boehnhardt, H., Sekanina, Z., Bonfils, X., Schütz, O., Beuzit, J.-L., Billeres, M., Garradd, G. J., Leisy, P., Marchis, F., Más, A., Origlia, L., Scarpa, D., Thomas, D., Tozzi, G. P., 2002. Split Comet C/2001 A2 (LINEAR). Earth Moon and Planets 90, 147–151.

Jenniskens, P., 2006. Meteor Showers and their Parent Comets. Cambridge University Press, Cambridge, UK.

Jenniskens, P., Blake, D. F., 1996. A mechanism for forming deep cracks in comets. Planet. Space Sci.44, 711–713.

Jewitt, D., 2004a. Looking through the HIPPO: Nucleus and dust in Comet 2P/Encke. Astron. J.128, 3061–3069.

Jewitt, D., Luu, J., 1989. A CCD portrait of Comet P/Tempel 2. Astron. J.97, 1766–1790.

Jewitt, D. C., 2004b. From cradle to grave: The rise and demise of the comets. In: Festou, M. H., Keller, U., Weaver, H. (Eds.), Comets II. University of Arizona Press, Tucson, pp. 659–676.

Jewitt, D. C., Meech, K. J., 1987. Surface brightness profiles of 10 comets. Astrophys. J.317, 992–1001.

Jockers, K., 1997. Observations of scattered light from cometary dust and their interpretation. Earth, Moon, Planets79, 221–245.

Jockers, K., Bonev, T., 1997. H_2O^+, CO^+, and dust in Comet P/Swift-Tuttle. Astron. Astrophys.319, 617–629.

Johnson, R. E., Cooper, J. F., Lanzerotti, L. J., Strazzulla, G., 1987. Radiation formation of a non-volatile comet crust. Astron. Astrophys.187, 889–892.

Jorda, L., Gutiérrez, P., 2000. Rotational properties of cometary nuclei. Earth, Moon, Planets89, 135–160.

Jorda, L., Hainaut, O., Smette, A., 1995. Photometric study of comets P/Faye 1991 XXI and Zanotta-Brewington 1992 III. Planet. Space Sci.43, 737–745.

Keller, H. U., 1990. Surface features and activity of the nucleus of Comet Halley. In: Comet Halley. Investigations, results, interpretations. Vol. 2. pp. 133–145.

Keller, H. U., Knollenberg, J., Markiewicz, W. J., 1994. Collimation of cometary dust jets and filaments. Planet. Space Sci.42, 367–382.

Keller, H. U., Küppers, M., Fornasier, S., Gutiérrez, P. J., Hviid, S. F., Jorda, L., Knollenberg, J., Lowry, S. C., Rengel, M., Bertini, I., Cremonese, G., Ip, W.-H., Koschny, D., Kramm, R., Kührt, E., Lara, L.-M., Sierks, H., Thomas, N., Barbieri, C., Lamy, P., Rickman, H., Rodrigo, R., A'Hearn, M. F., Angrilli, F., Barucci, M.-A., Bertaux, J.-L., da Deppo, V., Davidsson, B. J. R., de Cecco, M., Debei, S., Fulle, M., Gliem, F., Groussin, O., Lopez Moreno, J. J., Marzari, F., Naletto, G., Sabau, L., Sanz Andrés, A., Wenzel, K.-P., 2007. Observations of Comet 9P/Tempel 1 around the Deep Impact event by the OSIRIS cameras onboard Rosetta. Icarus 187, 87–103.

Keller, H. U., Skorov, Y. V., Markelov, G. N., 2004. Kinetic simulations of gas acitivity near a non-spherical cometary nucleus. Bull. Am. Ast. Soc.36, 1126.

Kelley, M. S., Woodward, C. E., Gehrz, R. D., Reach, W. T., 2004. Spitzer observations of Comet 2P/Encke: Six months post-perihelion. Bull. Am. Ast. Soc.36, 1434.

Kelley, M. S., Woodward, C. E., Jones, T. J., 2003. Infrared polarimetry of comets. Bull. Am. Ast. Soc.35, 987.

Kidger, M. R., 2003. Dust production and coma morphology of 67p/churyumov-gerasimenko during the 2002–2003 apparition. Astron. Astrophys.408, 767–774.

Kidger, M. R., 2004. Dust production and coma morphology of 67P/Churyumov-Gerasimenko during the 2002/2003 apparition. II. A comparative study of dust production in 46P/Wirtanen and 67P/Churyumov-Gerasimenko during their 2002/2003 apparition. Astron. Astrophys.420, 389–395.

Kidger, M. R., Serra-Ricart, M., Licandro, J., Torres, R., Schulman, L., Gonzalez-Perez, J. N., 1998. A jet-related colour change in the inner coma of comet Hale-Bopp (1995 O1)? Astron. Astrophys.329, 1152–1155.

Kirk, R. L., Duxbury, T. C., Hörz, F., Brownlee, D. E., Newburn, R. L., Tsou, P., The Stardust Team, 2005. Topography of the 81P/Wild 2 nucleus derived from Stardust stereo images. In: Mackwell, S., Stansbery, E. (Eds.), 36th Annual Lunar and Planetary Science Conference. Vol. 36 of Lunar and Planetary Institute Conference Abstracts. p. 2244.

Kiselev, N. N., Jockers, K., Bonev, T., 2004. CCD imaging polarimetry of Comet 2P/Encke. Icarus 168, 385–391.

Kissel, J., Brownlee, D. E., Buchler, K., Clark, B. C., Fechtig, H., Grun, E., Hornung, K., Igenbergs, E. B., Jessberger, E. K., Krueger, F. R., Kuczera, H., McDonnell, J. A. M., Morfill, G. M., Rahe, J., Schwehm, G. H., Sekanina, Z., Utterback, N. G., Volk, H. J., Zook, H. A., 1986. Composition of comet Halley dust particles from Giotto observations. Nature321, 336–337.

Kitamura, Y., 1986. Axisymmetric dusty gas jet in the inner coma of a comet. Icarus 66, 241–257.

Kitamura, Y., 1987. Axisymmetric dusty gas jet in the inner coma of a comet. II — The case of isolated jets. Icarus 72, 555–567.

Kitamura, Y., 1990. A numerical study of the interaction between two cometary jets — A possibility of shock formation in cometary atmospheres. Icarus 86, 455–475.

Klavetter, J. J., A'Hearn, M. F., 1994. An extended source for CN jets in Comet P/Halley. Icarus 107, 322–334.

Klinger, J., 1999. Thermal evolution of comet nuclei. Advances in Space Research 23, 1309–

1318.
Kolokolova, L., Jockers, K., 1997. Composition of cometary dust from polarization spectra. Planet. Space Sci.45, 1543–1550.
Krasnopolsky, V. A., Greenwood, J. B., Stancil, P. C., 2004. X-Ray and extreme ultraviolet emissions from comets. Space Science Reviews 113, 271–374.
Kresak, L., 1987. Dormant phases in the aging of periodic comets. Astron. Astrophys.187, 906–908.
Krolikowska, M., Sitarski, G., Szutowicz, S., 1998. Model of the nongravitational motion for Comet 32P/Comas Sola. Astron. Astrophys.335, 757–764.
Kronk, G. W., 1999. Cometography: A Catalog of Comets, Volume 1: Ancient–1799. Cambridge University Press, Cambridge, UK.
Kührt, E., Keller, H. U., 1994. The formation of cometary surface crusts. Icarus 109, 121–132.
Lamy, P. L., Toth, I., Grun, E., Keller, H. U., Sekanina, Z., West, R. M., 1996. Observations of Comet P/Faye 1991 XXI with the Planetary Camera of the Hubble Space Telescope. Icarus 119, 370–384.
Lamy, P. L., Toth, I., Jorda, L., Groussin, O., A'Hearn, M. F., Weaver, H. A., 2002. The nucleus of Comet 22P/Kopff and its inner coma. Icarus 156, 442–455.
Lamy, P. L., Toth, I., Weaver, H., Jorda, L., Kaasalainen, M., 2003. The nucleus of Comet 67P/Churyumov-Gerasimenko, the new target of the Rosetta mission. Bull. Am. Ast. Soc.35, 970.
Lamy, P. L., Toth, I., Weaver, H. A., 1998. Hubble Space Telescope observations of the nucleus and inner coma of Comet 19P/1904 Y2 (Borrelly). Astron. Astrophys.337, 945–954.
Lamy, P. L., Toth, I., Weaver, H. A., Jorda, L., Kaasalainen, M., Gutiérrez, P. J., 2006. Hubble Space Telescope observations of the nucleus and inner coma of Comet 67P/Churyumov-Gerasimenko. Astron. Astrophys.458, 669–678.
Lara, L., Rodrigues, P., Rodrigo, R., Boehnhardt, H., Bonev, T., Borisov, G., 2007. Comet 73p/schwassmann-wachmann. IAU Circ. 8708.
Lara, L. M., Boehnhardt, H., Gredel, R., Gutiérrez, P. J., Ortiz, J. L., Rodrigo, R., Vidal-Nuñez, M. J., 2006. Pre-impact monitoring of Comet 9P/Tempel 1, the Deep Impact target. Astron. Astrophys.445, 1151–1157.
Lara, L. M., Boehnhardt, H., Gredel, R., Gutiérrez, P. J., Rodrigo, R., Vidal-Nuñez, M. J., 2007. Behavior of Comet 9P/Tempel 1 around the Deep Impact event. Astron. Astrophys.465, 1061–1067.
Lara, L. M., de León, J., Licandro, J., Gutiérrez, P. J., 2005. Dust activity in Comet 67P/Churyumov-Gerasimenko from February 20 to April 20, 2003. Earth, Moon, Planets97, 165–175.
Lara, L.-M., Tozzi, G. P., Boehnhardt, H., DiMartino, M., Schulz, R., 2004. Gas and dust in Comet C/2000 WM1 during its closest approach to Earth: Optical imaging and long-slit spectroscopy. Astron. Astrophys.422, 717–729.
Larson, S. M., Slaughter, C. M., 1992. Evaluating some computer enhancement algorithms that improve the visibility of cometary morphology. In: Harris, A., Bowell, E. (Eds.), Asteroids, Comets, Meteors, 1991. Lunar and Plantary Institute, Houston, pp. 337–343.
Laufer, D., Pat-El, I., Bar-Nun, A., 2005. Experimental simulation of the formation of non-circular active depressions on Comet Wild 2 and of ice grain ejection from cometary

surfaces. Icarus 178, 248–252.
Lecacheux, A., Biver, N., Crovisier, J., Bockelée-Morvan, D., Baron, P., Booth, R. S., Encrenaz, P., Florén, H.-G., Frisk, U., Hjalmarson, Å., Kwok, S., Mattila, K., Nordh, L., Olberg, M., Olofsson, A. O. H., Rickman, H., Sandqvist, A., von Schéele, F., Serra, G., Torchinsky, S., Volk, K., Winnberg, A., 2003. Observations of water in comets with Odin. Astron. Astrophys.402, L55–L58.
Lederer, S. M., Campins, H., 2002. Evidence for chemical heterogeneity in the nucleus of C/1995 O1 (Hale-Bopp). Earth, Moon, Planets90, 381–389.
Levasseur-Regourd, A.-C., 1999. Polarization of light scattered by cometary dust particles: Observations and tentative interpretations. Space Science Reviews 90, 163–168.
Levasseur-Regourd, A. C., Goidet, B., Le Duin, T., Malique, C., Renard, J. B., Bertaux, J. L., 1993. Short Communication: Optical probing of dust in Comet Grigg-Skjellerup from the Giotto spacecraft. Planet. Space Sci.41, 167–169.
Licandro, J., Tancredi, G., Lindgren, M., Rickman, H., Hutton, R. G., 2000. CCD photometry of cometary nuclei, I: Observations from 1990-1995. Icarus 147, 161–179.
Lien, D., 2002. Differences in dynamical dust properties between young and old comets. Bull. Am. Ast. Soc.34, 869.
Lin, Z. Y., Weiler, M., Rauer, H., Ip, W. H., 2007. Photometry and imaging of comet C/2004 Q2 (Machholz) at Lulin and La Silla. Astron. Astrophys.469, 771–776.
Luu, J. X., Jewitt, D. C., 1992. Near-aphelion CCD photometry of Comet P/Schwassmann-Wachmann 2. Astron. J.104, 2243–2249.
Mäkinen, J. T. T., Combi, M. R., Bertaux, J.-L., Quémerais, E., Schmidt, W., 2007. SWAN observations of 9P/Tempel 1 around the Deep Impact event. Icarus 187, 109–112.
Manfroid, J., Hutsemékers, D., Jehin, E., Cochran, A. L., Arpigny, C., Jackson, W. M., Meech, K. J., Schulz, R., Zucconi, J.-M., 2007. The impact and rotational light curves of Comet 9P/Tempel 1. Icarus 187, 144–155.
McBride, N., Green, S. F., Chantal Levasseur-Regourd, A., Goidet-Devel, B., Renard, J.-B., 1997. The inner dust coma of Comet 26P/Grigg-Skjellerup: Multiple jets and nucleus fragments? Mon. Not. R. Astron. Soc.289, 535–553.
McFadden, L. A., Crockett, C. J., Wellnitz, D. D., Feaga, L. M., A'Hearn, M. F., Farnham, T. L., Groussin, O., Li, J.-Y., Lisse, C. M., Sunshine, J. M., Delamere, A., Klaasen, K. P., 2006. Gas and dust imaging of the inner coma of 9P/Tempel 1 before and after impact. Bull. Am. Ast. Soc.38, 1704.
Mendis, D. A., Brin, G. D., 1977. Monochromatic brightness variations of comets. II — Core-mantle model. Moon 17, 359–372.
Mikuz, H., 1994. Comet Machholz (1994o). IAU Circ. 6055.
Milani, G. A., Szabó, G. M., Sostero, G., Trabatti, R., Ligustri, R., Nicolini, M., Facchini, M., Tirelli, D., Carosati, D., Vinante, C., Higgins, D., 2007. Photometry of Comet 9P/Tempel 1 during the 2004/2005 approach and the Deep Impact module impact. Icarus 187, 276–284.
Miura, N., Ishiguro, M., Sarugaku, Y., Ueno, M., 2007. New approach to study non-gravitational motion of a comet normal to the orbital plane. PASJ59, L7–L10.
Montalto, M., Riffeser, A., Hopp, U., Wilke, S., Carraro, G., 2008. The Comet 17P/Holmes 2007 outburst: The early motion of the outburst material. Astron. Astrophys.479, L45–L49.
Moreno, F., Ortiz, J. L., Santos-Sanz, P., Morales, N., Vidal-Núñez, M. J., Lara, L. M.,

Gutiérrez, P. J., 2008. A model of the early evolution of the 2007 outburst of Comet 17P/Holmes. Astrophys. J. Lett.677, L63–L66.

Mueller, B. E. A., Ferrin, I., 1996. Change in the rotational period of Comet P/Tempel 2 between the 1988 and 1994 apparitions. Icarus 123, 463–477.

Mueller, B. E. A., Samarasinha, N. H., 2002. Visible lightcurve observations of Comet 19p/Borrelly. Earth, Moon, Planets90, 463–471.

Ninkov, Z., 1994. A near stellar occultation by P/Grigg-Skjellerup. Astron. J.107, 1182–1188.

Orosei, R., Capaccioni, F., Capria, M. T., Coradini, A., Espinasse, S., Federico, C., Salomone, M., Schwehm, G. H., 1995. Gas and dust emission from a dusty porous comet. Astron. Astrophys.301, 613–627.

Palmer, P., de Pater, I., Snyder, L. E., 1989. VLA observations of the OH emission from Comet Wilson (1986l) - The value of high resolution in both spatial and velocity coordinates. Astron. J.97, 1791–1797.

Pansecchi, L., Fulle, M., Sedmak, G., 1987. The nature of two anomalous structures observed in the dust tail of Comet Bennett 1970. II — A possible neck-line structure. Astron. Astrophys.176, 358–366.

Prialnik, D., Benkhoff, J., Podolak, M., 2004. Modeling the structure and activity of comet nuclei. In: Festou, M. H., Keller, U., Weaver, H. (Eds.), Comets II. University of Arizona Press, Tucson, pp. 359–387.

Prialnik, D., Egozi, U., Ban-Nun, A., Podolak, M., Greenzweig, Y., 1993. On pore size and fracture in gas-laden comet nuclei. Icarus 106, 499–507.

Rabinowitz, D. L., 1988. A source map for dust jets observed in the coma of Comet P/Halley. Astron. Astrophys.200, 225–247.

Rahe, J., Donn, B., Wurm, K., 1969. Atlas of cometary forms. NASA Special Publication 198.

Ramos-Larios, G., Phillips, J. P., Kemp, S. N., Toledo-Roy, J. C., 2008. Near-infrared mapping of comet 73P/Schwassmann-Wachmann 3-B. Mon. Not. R. Astron. Soc.384, 630–636.

Randall, C. E., Schleicher, D. G., Ballou, R. G., Osip, D. J., 1992. Observational constraints on molecular scalelengths and lifetimes in comets. Bull. Am. Ast. Soc.24, 1002.

Reach, W. T., Kelley, M. S., Sykes, M. V., 2007. A survey of debris trails from short-period comets. Icarus 191, 298–322.

Renard, J.-B., Hadamcik, E., Levasseur-Regourd, A.-C., 1996. Polarimetric CCD imaging of comet 47P/Ashbrook-Jackson and variability of polarization in the inner coma of comets. Astron. Astrophys.316, 263–269.

Richardson, J. E., Melosh, H. J., Lisse, C. M., Carcich, B., 2007. A ballistics analysis of the Deep Impact ejecta plume: Determining Comet Tempel 1's gravity, mass, and density. Icarus 190, 357–390.

Rickman, H., 1991. The thermal history and structure of cometary nuclei. In: Newburn, Jr., R. L., Neugebauer, M., Rahe, J. (Eds.), IAU Colloq. 116: Comets in the post-Halley era. Vol. 167 of Astrophysics and Space Science Library. pp. 733–760.

Rickman, H., Kamel, L., Froeschle, C., Festou, M. C., 1991. Nongravitational effects and the aging of periodic comets. Astron. J.102, 1446–1463.

Rickman, H., Sitarski, G., Todorovic-Juchniewicz, B., 1987. Nongravitational motion of Comet P/Kopff during 1958-1983. Astron. Astrophys.188, 206–211.

Rodionov, A. V., Crifo, J.-F., 2006. Time-dependent, three-dimensional fluid model of the

outer coma, with application to the comet Hale-Bopp gas spirals. Advances in Space Research 38, 1923–1927.

Rodionov, A. V., Jorda, L., Jones, G. H., Crifo, J. F., Colas, F., Lecacheux, J., 1998. Comet Hyakutake gas arcs: First observational evidence of standing shock waves in a cometary coma. Icarus 136, 232–267.

Rousselot, P., Vernotte, F., Clairemidi, J., Moreels, G., 1992. Evidence for two types of sources creating Halley's coma. In: Guyenne, T. D., Hunt, J. J. (Eds.), Environment Observation and Climate Modelling Through International Space Projects. pp. 211–212.

Samarasinha, N. H., Larson, S., Beshore, E., 2006. Application of image enhancement techniques to comets: A critical analysis . Bull. Am. Ast. Soc.38, 537.

Samarasinha, N. H., Mueller, B. E. A., 2002. Spin axis direction of Comet 19P/Borrelly based on observations from 2000 and 2001. Earth, Moon, Planets90, 473–482.

Sarugaku, Y., Ishiguro, M., Pyo, J., Miura, N., Nakada, Y., Usui, F., Ueno, M., 2007. Detection of a long-extended dust trail associated with short-period Comet 4P/Faye in 2006 return. PASJ59, L25–L28.

Schleicher, D. G., 2006. Compositional and physical results for Rosetta's new target Comet 67P/Churyumov Gerasimenko from narrowband photometry and imaging. Icarus 181, 442–457.

Schleicher, D. G., 2007. Deep Impact's target Comet 9P/Tempel 1 at multiple apparitions: Seasonal and secular variations in gas and dust production. Icarus 190, 406–422.

Schleicher, D. G., Barnes, K. L., Baugh, N. F., 2006. Photometry and imaging results for Comet 9P/Tempel 1 and Deep Impact: Gas production rates, postimpact light curves, and ejecta plume morphology. Astron. J.131, 1130–1137.

Schleicher, D. G., Farnham, T. L., 2004. Photometry and imaging of the coma with narrowband filters. In: Festou, M. H., Keller, U., Weaver, H. (Eds.), Comets II. University of Arizona Press, Tucson, pp. 449–469.

Schleicher, D. G., Millis, R. L., Osip, D. J., Lederer, S. M., 1998. Activity and the rotation period of Comet Hyakutake (1996 B2). Icarus 131, 233–244.

Schleicher, D. G., Woodney, L., 2007a. Comet 8P/Tuttle. IAU Circ. 8903.

Schleicher, D. G., Woodney, L., 2007b. Comet 8P/Tuttle. IAU Circ. 8906.

Schleicher, D. G., Woodney, L. M., Millis, R. L., 2003. Comet 19P/Borrelly at multiple apparitions: seasonal variations in gas production and dust morphology. Icarus 162, 415–442.

Schloerb, F. P., Lovell, A. J., 1998. Modelling of HCN emission from Comets Hyakutake and Hale-Bopp. Bull. Am. Ast. Soc.30, 1073.

Schlosser, W., Schulz, R., Koczet, P., 1986. The cyan shells of Comet P/Halley. In: ESLAB Symposium on the Exploration of Halley's Comet. Volume 1: Plasma and Gas. Vol. 250 of ESA Special Publication. pp. 495–498.

Schulz, R., 2002. Comparative study of gas coma morphologies. In: Warmbein, B. (Ed.), Asteroids, Comets, and Meteors: ACM 2002. Vol. 500 of ESA Special Publication. pp. 553–556.

Schulz, R., 2008. Morphology composition isotopes: Recent results from observations. Space Science Reviews, In Press.

Schulz, R., Stüwe, J. A., Boehnhardt, H., Gaessler, W., Tozzi, G. P., 2003. Characterization of STARDUST target comet 81P/Wild 2 from 1996 to 1998. Astron. Astrophys.398, 345–

352.
Schulz, R., Stüwe, J., 2000. Characterization of STARDUST target Comet 81P/Wild 2 from 1996 observations. Bull. Am. Ast. Soc.32, 1076.
Schulz, R., Stüwe, J. A., 2002. The dust coma of Comet C/1999 S4 (LINEAR). Earth, Moon, Planets90, 195–203.
Schulz, R., Stüwe, J. A., Böhnhardt, H., 2004. Monitoring Comet 67P/Churyumov-Gerasimenko from ESO in 2003. In: Colangeli, L., Mazzotta Epifani, E., Palumbo, P. (Eds.), The New Rosetta Targets. Observations, Simulations and Instrument Performances. Vol. 311 of Astrophysics and Space Science Library. pp. 15–24.
Schulz, R., Stüwe, J. A., Erd, C., 2005. Coma morphology of three non-periodic comets. Earth, Moon, Planets97, 387–397.
Schwarz, G., Cosmovici, C. B., Mack, P., Ip, W.-H., 1989. Image processing techniques for gas morphology studies in the coma of Comet Halley. Adv. Space Res. 9, 217–220.
Seiferlin, K., Spohn, T., Benkhoff, J., 1995. Cometary ice texture and the thermal evolution of comets. Advances in Space Research 15, 35–38.
Sekanina, Z., 1974. On the nature of the anti-tail of Comet Kohoutek 1973f. I — A working model. Icarus 23, 502–518.
Sekanina, Z., 1981. Distribution and activity of discrete emission areas on the nucleus of periodic Comet Swift-Tuttle. Astron. J.86, 1741–1773.
Sekanina, Z., 1984. Precession model for the nucleus of periodic Comet Kopff. Astron. J.89, 1573–1586.
Sekanina, Z., 1987a. Anisotropic emission from comets: Fans versus jets. 1: Concept and modeling. In: Rolfe, E. J., Battrick, B. (Eds.), Diversity and Similarity of Comets. Vol. 278 of ESA Special Publication. pp. 315–322.
Sekanina, Z., 1987b. Anisotropic emission from comets: Fans versus jets. 2: Periodic Comet Tempel 2. In: Rolfe, E. J., Battrick, B. (Eds.), Diversity and Similarity of Comets. Vol. 278 of ESA Special Publication. pp. 323–336.
Sekanina, Z., 1988a. Outgassing asymmetry of periodic comet Encke. I - Apparitions 1924-1984. Astron. J.95, 911–924.
Sekanina, Z., 1988b. Outgassing asymmetry of periodic Comet Encke. II - Apparitions 1868-1918 and a study of the nucleus evolution. Astron. J.96, 1455–1475.
Sekanina, Z., 1988. Periodic Comet Tempel 2 (1987g). IAU Circ. 4624.
Sekanina, Z., 1989. Nuclei of two earth-grazing comets of fan-shaped appearance. Astron. J.98, 2322–2345.
Sekanina, Z., 1990. Gas and dust emission from comets and life spans of active areas on their rotating nuclei. Astron. J.100, 1293–1314.
Sekanina, Z., 1991a. Cometary activity, discrete outgassing areas, and dust-jet formation. In: Newburn, Jr., R. L., Neugebauer, M., Rahe, J. (Eds.), IAU Colloq. 116: Comets in the post-Halley era. Vol. 167 of Astrophysics and Space Science Library. pp. 769–823.
Sekanina, Z., 1991b. Comprehensive model for the nucleus of periodic Comet Tempel 2 and its activity. Astron. J.102, 350–388.
Sekanina, Z., 1991c. Randomization of dust-ejecta motions and the observed morphology of cometary heads. Astron. J.102, 1870–1878.
Sekanina, Z., 2003. A model for comet 81P/Wild 2. J. Geophys. Res. (Planets)108 (E10), 8112.

Sekanina, Z., 2007. Earth's 2006 encounter with comet 73P/Schwassmann-Wachmann: Products of nucleus fragmentation seen in closeup. In: Valsecchi, G. B., Vokrouhlický, D. (Eds.), IAU Symposium. Vol. 236 of IAU Symposium. pp. 211–220.

Sekanina, Z., 2008. Exploding Comet 17P/Holmes. International Comet Quarterly 30, 3–28.

Sekanina, Z., Brownlee, D. E., Economou, T. E., Tuzzolino, A. J., Green, S. F., 2004. Modeling the nucleus and jets of Comet 81P/Wild 2 based on the Stardust encounter data. Science 304, 1769–1774.

Sitarski, G., 1994. The nongravitational motion of Comet P/Kopff during 1906–1991. Acta Astronomica 44, 417–426.

Skorov, Y. V., Keller, H. U., Jorda, L., Davidsson, B. J. R., 2002. Thermophysical modelling of Comet P/Borrelly effects of volume energy absorption and volume sublimation. Earth, Moon, Planets90, 293–303.

Skorov, Y. V., Rickman, H., 1995. A kinetic model of gas flow in a porous cometary mantle. Planet. Space Sci.43, 1587–1594.

Smoluchowski, R., 1989. Properties of mantles on cometary nuclei. Astron. J.97, 241–245.

Snodgrass, C., Fitzsimmons, A., Boehnhardt, H., Lister, T., Naylor, T., Bell, C., Colas, F., Lecacheux, J., Sostero, G., Guido, E., Young, J., McGaha, J., 2007. Comet 17P/Holmes. Central Bureau Electronic Telegrams 1111.

Soderblom, L. A., Becker, T. L., Bennett, G., Boice, D. C., Britt, D. T., Brown, R. H., Buratti, B. J., Isbell, C., Giese, B., Hare, T., Hicks, M. D., Howington-Kraus, E., Kirk, R. L., Lee, M., Nelson, R. M., Oberst, J., Owen, T. C., Rayman, M. D., Sandel, B. R., Stern, S. A., Thomas, N., Yelle, R. V., 2002. Observations of Comet 19P/Borrelly by the miniature integrated camera and spectrometer aboard Deep Space 1. Science 296, 1087–1091.

Soderblom, L. A., Boice, D. C., Britt, D. T., Brown, R. H., Buratti, B. J., Kirk, R. L., Lee, M., Nelson, R. M., Oberst, J., Sandel, B. R., Stern, S. A., Thomas, N., Yelle, R. V., 2004. Imaging Borrelly. Icarus 167, 4–15.

Spinrad, H., 1991. Systematic displacements between gas and dust in the sunward fans of two low-activity comets. Astron. J.102, 1207–1212.

Storm, S., Samarasinha, N., Mueller, B., Farnham, T., Fernandez, Y., Kidder, A., Snowden, D., A'Hearn, M., Harris, W., Knight, M., Morgenthaler, J., Lisse, C., Roesler, F., 2006. Constraining the rotational period for component C of the periodic Comet 73P/Schwassmann-Wachmann 3. Bull. Am. Ast. Soc.38, 935.

Strazzulla, G., Johnson, R. E., 1991. Irradiation effects on comets and cometary debris. In: Newburn, Jr., R. L., Neugebauer, M., Rahe, J. (Eds.), IAU Colloq. 116: Comets in the post-Halley era. Vol. 167 of Astrophysics and Space Science Library. pp. 243–275.

Sunshine, J. M., A'Hearn, M. F., Groussin, O., Li, J.-Y., Belton, M. J. S., Delamere, W. A., Kissel, J., Klaasen, K. P., McFadden, L. A., Meech, K. J., Melosh, H. J., Schultz, P. H., Thomas, P. C., Veverka, J., Yeomans, D. K., Busko, I. C., Desnoyer, M., Farnham, T. L., Feaga, L. M., Hampton, D. L., Lindler, D. J., Lisse, C. M., Wellnitz, D. D., 2006. Exposed water ice deposits on the surface of Comet 9P/Tempel 1. Science 311, 1453–1455.

Sunshine, J. M., Groussin, O., Schultz, P. H., A'Hearn, M. F., Feaga, L. M., Farnham, T. L., Klaasen, K. P., 2007. The distribution of water ice in the interior of Comet Tempel 1. Icarus 190, 284–294.

Suzuki, B., Kurihara, H., Watanabe, J., 1993. Gaseous jets of P/Hartley 2. LPI Contributions

810, 285.
Suzuki, B., Kurihara, H., Watanabe, J.-I., 1990. Detection of C_2 jets of Comet Austin 1989c1. PASJ42, L93–L97.
Sykes, M. V., 1988. IRAS observations of extended zodiacal structures. Astrophys. J. Lett.334, L55–L58.
Szabó, G. M., Kiss, L. L., Sárneczky, K., Sziládi, K., 2002. Spectrophotometry and structural analysis of 5 comets. Astron. Astrophys.384, 702–710.
Szegö, K., Crifo, J.-F., Rodionov, A. V., Fulle, M., 2002. The near-nuclear coma of Comet Halley in March 1986. Earth, Moon, Planets90, 435–443.
Tancredi, G., Fernández, J. A., Rickman, H., Licandro, J., 2000. A catalog of observed nuclear magnitudes of Jupiter family comets. Astron. Astrophys. Supp.146, 73–90.
Tancredi, G., Fernández, J. A., Rickman, H., Licandro, J., 2006. Nuclear magnitudes and the size distribution of Jupiter family comets. Icarus 182, 527–549.
Tauber, F., Kührt, E., 1987. Thermal stresses in cometary nuclei. Icarus 69, 83–90.
Telesco, C. M., Decher, R., Baugher, C., Campins, H., Mozurkewich, D., Thronson, H. A., Cruikshank, D. P., Hammel, H. B., Larson, S., Sekanina, Z., 1986. Thermal-infrared and visual imaging of comet Giacobini-Zinner. Astrophys. J. Lett.310, L61–L65.
Thiel, K., Koelzer, G., Kochan, H., Gruen, E., Kohl, H., 1991. New results of the dust investigations in the comet simulation project KOSI. In: Ryder, G., Sharpton, V. L. (Eds.), Lunar and Planetary Science Conference. Vol. 21 of Lunar and Planetary Science Conference. pp. 579–589.
Thiel, K., Koelzer, G., Kochan, H., Ratke, L., Gruen, E., Koehl, H., 1989. Dynamics of crust formation and dust emission of comet nucleus analogues under isolation. In: Hunt, J. J., Guyenne, T. D. (Eds.), Physics and Mechanics of Cometary Materials. Vol. 302 of ESA Special Publication. pp. 221–225.
Thomas, N., A'Hearn, M. F., Boice, D. C., Britt, D. T., Meech, K. J., Sandel, B. R., Soderblom, L. A., Yelle, R. V., 2001. Jet morphology in the inner coma of Comet 19P/Borrelly observed by the Deep Space One MICAS imaging system. Bull. Am. Ast. Soc.33, 1074.
Thomas, P. C., Veverka, J., Belton, M. J. S., Hidy, A., A'Hearn, M. F., Farnham, T. L., Groussin, O., Li, J.-Y., McFadden, L. A., Sunshine, J., Wellnitz, D., Lisse, C., Schultz, P., Meech, K. J., Delamere, W. A., 2007. The shape, topography, and geology of Tempel 1 from Deep Impact observations. Icarus 187, 4–15.
Tozzi, G. P., Cimatti, A., di Serego Alighieri, S., Cellino, A., 1997. Imaging polarimetry of comet C/1996 B2 (Hyakutake) at the perigee. Planet. Space Sci.45, 535–540.
Tozzi, G. P., Lara, L. M., Kolokolova, L., Boehnhardt, H., Licandro, J., Schulz, R., 2004. Sublimating components in the coma of comet C/2000 WM_1 (LINEAR). Astron. Astrophys.424, 325–330.
Trigo-Rodriguez, J. M., Davidsson, B., Montanes-Rodriguez, P., Sanchez, A., Troughton, B., 2008. All-sky cameras detection and telescope follow-up of the 17P/Holmes outburst. In: Lunar and Planetary Institute Conference Abstracts. Vol. 39 of Lunar and Planetary Institute Conference Abstracts. pp. 1627–1628.
Vaisberg, O. L., Smirnov, V., Omel'Chenko, A., Gorn, L., Iovlev, M., 1987. Spatial and mass distribution of low-mass dust particles ($m < 10^{-10}$ g) in comet P/Halley's coma. Astron. Astrophys.187, 753–760.

Vasundhara, R., Chakraborty, P., 2004. Investigations of the rotation pole from the morphology of dust fans of Comet 81P/Wild 2. Astrophys. J.616, 1278–1283.

Veal, J. M., Snyder, L. E., Wright, M., Woodney, L. M., Palmer, P., Forster, J. R., de Pater, I., A'Hearn, M. F., Kuan, Y.-J., 2000. An interferometric study of HCN in Comet Hale-Bopp (C/1995 O1). Astron. J.119, 1498–1511.

Vergazov, M. A., Krasnobaev, K. V., 1985. Axisymmetric flow of reacting gas from a comet nucleus. Soviet Astronomy Letters 11, 232–235.

Waldemarsson, K. W. T., Kolokolova, L., Gustafson, B. A. S., 2000. Are there dust-flakes in cometary atmospheres? Bull. Am. Ast. Soc.32, 1486.

Walker, R. G., Campins, H., Schlapfer, M., 1992. High resolution images of P/Tempel 1 and P/Tempel 2 constructed from IRAS survey data. In: Harris, A. W., Bowell, E. (Eds.), Asteroids, Comets, Meteors 1991. pp. 617–620.

Wallis, M. K., 1982. Dusty gas-dynamics in real comets. In: Wilkening, L. L. (Ed.), Comets. Univ. of Arizona Press, Tucson, pp. 357–369.

Weaver, H. A., Stern, S. A., Parker, J. W., 2003. Hubble Space Telescope STIS observations of Comet 19P/Borrelly during the Deep Space 1 encounter. Astron. J.126, 444–451.

Weiler, M., Rauer, H., Helbert, J., 2004. Optical observations of Comet 67P/Churyumov-Gerasimenko. Astron. Astrophys.414, 749–755.

Weiler, M., Rauer, H., Knollenberg, J., Sterken, C., 2007. The gas production of Comet 9P/Tempel 1 around the Deep Impact date. Icarus 190, 423–431.

Welch, P. G., 2003. Matching cometary ejection processes to the Leonids 1998-2001 using a hybrid numerical model. Mon. Not. R. Astron. Soc.342, 971–994.

Wetherill, G. W., 1991. End products of cometary evolution — Cometary origin of earth-crossing bodies of asteroidal appearance. In: Newburn, Jr., R. L., Neugebauer, M., Rahe, J. (Eds.), IAU Colloq. 116: Comets in the post-Halley era. Vol. 167 of Astrophysics and Space Science Library. pp. 537–556.

Whipple, F. L., 1978. Cometary brightness variation and nucleus structure. Moon and Planets 18, 343–359.

Woodney, L., Schleicher, D. G., Reetz, K. M., Ryan, K. J., 2007. Rotational properties of Comet 2P/Encke based on nucleus lightcurves and coma morphology. Bull. Am. Ast. Soc.39, 486.

Woodney, L. M., Barnes, K. L., Baugh, N. F., Schleicher, D. G., 2005. Gas and dust morphological results from narrowband imaging of Deep Impact's target Comet 9P/Tempel 1. Bull. Am. Ast. Soc.37, 647.

Yelle, R. V., Soderblom, L. A., Jokipii, J. R., 2004. Formation of jets in Comet 19P/Borrelly by subsurface geysers. Icarus 167, 30–36.

Yeomans, D. K., Chodas, P. W., 1989. An asymmetric outgassing model for cometary non-gravitational accelerations. Astron. J.98, 1083–1093.

Yeomans, D. K., Giorgini, J. D., Chesley, S. R., 2005. The history and dynamics of Comet 9P/Tempel 1. Space Science Reviews 117, 123–135.